

Comparison of velocity and turbulence profiles downstream of perforated plate flow conditioners

E. P. Spearman, J. A. Sattary and M. J. Reader-Harris

National Engineering Laboratory, East Kilbride, G75 0GU, Scotland, UK

Received 15 July 1996

This paper presents the results obtained when placing different designs of perforated plate flow conditioner downstream of two common flow-disturbing installations in turn: a single 90° bend and a twisted S bend. The results comprise a series of LDV measurements of velocity and r.m.s. fluctuation velocity profiles made in two perpendicular planes at locations between 3 and 41 pipe diameters (D) downstream of the conditioners. The flow conditioners were placed at $4D$ downstream of the flow-disturbing installations. Measurements were also made without the inclusion of a flow conditioner for comparison. Several designs of flow conditioner give profiles within 5% of a fully developed profile $11D$ downstream of the conditioner; so significant reductions in lengths of meter runs should be possible. The Spearman (NEL) design performs at least as well as other contemporary designs and is available for inclusion in the relevant standards. These measurements were carried out in a water pipeline. © 1997 Elsevier Science Ltd.

Keywords: LDV; flow conditioning; velocity profiles

Nomenclature

D	pipe diameter
d	orifice plate throat diameter
K	head loss coefficient
ΔP	differential pressure
R	radius of bend
x	distance from pipe axis in horizontal plane
y	distance from pipe axis in vertical plane
U	mean pipe velocity
u	axial velocity
u'	axial root mean square fluctuation velocity
α	porosity
β	diameter ratio for an orifice plate, d/D
ρ	density

1. Introduction

Although flow conditioning for closed conduits has been an established practice for many years, the emergence of the perforated plate conditioner has been a relatively recent event. Much of the motivation for this has come from those seeking to improve flow metering using differential pressure meters (especially orifice plates) by updating and improving the relevant standards, for instance ISO 5167-1 (BS 1042: 1.1) [1, 2].

It has become apparent that those parts of the

ISO standard dealing with flow conditioning devices are in urgent need of revision. The first problem is that the flow conditioners allowed by the standard (the tube bundle, Sprengle, étoile, AMCA and Zanker conditioners) must be installed with a minimum of $20D$ between the conditioner and flow-disturbing installation, and $22D$ between the flow conditioner and the orifice plate. This requirement of $42D$ is greater than many of the ISO standard's own straight length requirements for cases without conditioners, whereas various researchers have shown that good results can be achieved with much reduced distances [3-5].

Another problem is that single perforated plate flow conditioners are not included in the ISO standard. This is despite the fact that the best designs provide better flow conditioning than those conditioners included in the ISO standard besides being more easily manufactured and installed. One reason for this absence is that many of the best designs have been patented which makes it difficult for these designs to be included in the standards. It is certainly possible to reduce significantly the straight length requirements of ISO 5167-1: such a change would encourage industries that require accurate flow measurement to use effective flow conditioners and thus allow a sizeable reduction in the overall cost and space requirements of flow metering especially offshore.

The purpose of this project, therefore, was to design a perforated plate flow conditioner with a performance at least as good if not better than any designs

available at present. The design would then be introduced to the public domain which would make it easily available for inclusion in the standards. A number of conditioners were tested and the conditioner causing the flow to return to a fully developed profile over the shortest length of pipe could be identified.

2. Description of the devices tested

Initially three conditioners were chosen which had different design aspects. These were the Mitsubishi Heavy Industries (MHI) conditioner and two different designs of the Laws conditioner.

2.1. The MHI conditioner

This design has been in general use for some years now [6] and is shown in Figure 1. It consists of 35 holes positioned so that the resistance is graded across the conditioner in such a manner as to allow more flow through the centre than at the edge. This helps in trying to produce the form of the fully developed flow profile. The porosity (α), equal to the ratio of the total area of hole space across the flow conditioner to the total cross-sectional area of the pipe, is approximately 59%. This gives rise to a head loss coefficient (K) typically in the range 1–1.7 depending on whether an upstream chamfer is used. MHI showed that after placing the conditioner $2D$ downstream of a twisted S bend, no shift in discharge coefficient could be expected when placing a $\beta=0.8$ orifice plate at least $8D$ downstream of the conditioner. Independent tests by Humphreys and Hobbs [5] obtained a shift in discharge coefficient of -0.5% with the conditioner located $2D$ downstream of a twisted S bend and $10D$ between the conditioner and an orifice plate of $\beta=0.8$.

However, they also showed that with a single bend replacing the twisted S bend in a similar meter run, a shift of $+1\%$ was obtained which has led to the conclusion that while performing relatively well in swirling flows this conditioner is not as efficient at removing asymmetry.

2.2. The Laws conditioners

In recent years the Laws design of flow conditioner has come to the fore. It comprises a relatively large central hole surrounded by an inner ring of smaller holes, in turn surrounded by an outer ring of even smaller holes. The original Laws design [7] was based around a value of K equal to 2.7 proposed by Elder [8] to eliminate non-uniformities using plane wire gauze screens. This value caused the porosity to be set at 51.55%. Laws proposed a range of conditioners containing various numbers of holes in the inner and outer rings, but has specifically recommended a 1–7–13 arrangement. Laws [7] compared velocity profiles measured downstream of the conditioner, which had been placed $3D$ downstream of various flow disturbing installations, with the 5% rule from ISO 5167-1 Clause 7.4 (which states that 'acceptable velocity profiles can be presumed to exist when, at each point across the pipe section, the ratio of local axial velocity to the maximum axial velocity at the cross-section agrees to within 5% with that which would be achieved in swirl-free flow at the same radial position at a cross-section located at the end of a very long straight length, $>100D$, of similar pipe, i.e. fully developed flow') and found that the most disturbed upstream flow studied satisfied the ISO Clause at $8.5D$ downstream of the conditioner. Sanderson and Sweetland [9] and Lake and Reid [10] found the Laws conditioner to

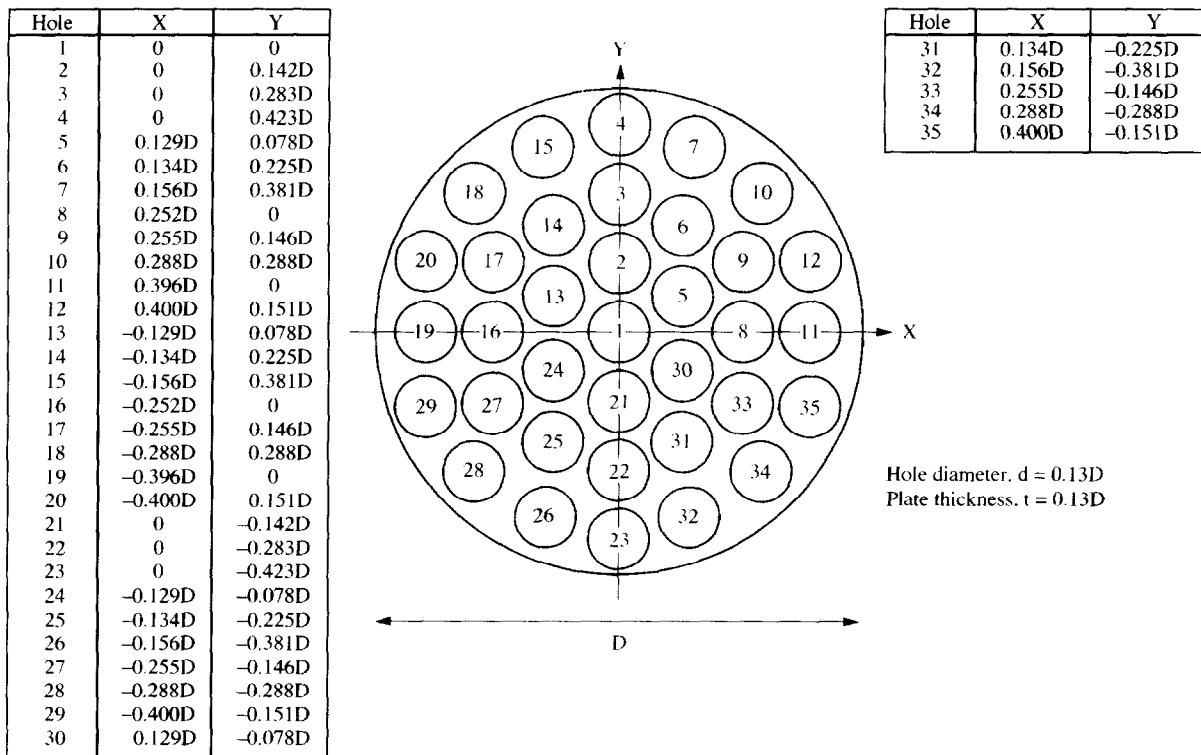


Figure 1 The MHI flow conditioner

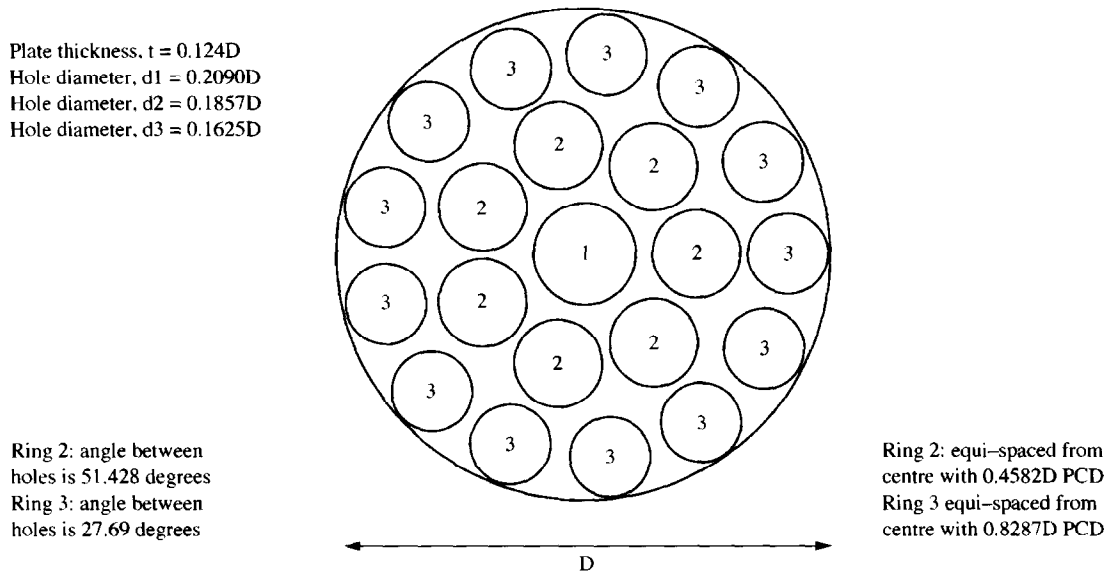


Figure 2 The unchamfered Laws flow conditioner

perform best in their comparisons with other flow conditioners. Further improvements have since been made to the original design and the two conditioners tested were:

1. A Laws conditioner with an unchamfered upstream face and a porosity of $\alpha=62.85\%$ (Figure 2).
2. A Laws conditioner with an upstream chamfer of 1 mm at 45° and a porosity of $\alpha=52.2\%$ (Figure 3).

2.3. The spearman (NEL) conditioner

Work also took place at NEL on a new perforated plate design. The final version is shown in Figure 4. It contains an outer ring of 16 holes, an inner ring of eight holes and four holes arranged in a square at the centre. The porosity of the conditioner is 47.5%. The conditioner was designed to have a value of K close

to 2.7, a high degree of rotational symmetry and a graded resistance across the conditioner.

3. Experimental set-up

The conditioners were tested by placing them downstream of two very common pipe installations in turn:

1. a single 90° swept bend with a bend radius to pipe diameter ratio (R/D) of 1.5 producing an asymmetric flow with counter-rotating vortices, and
2. a twisted S bend comprising two of the above bends placed in perpendicular planes producing a swirling flow coupled with asymmetry. Because of the use of weld-neck flanges the distance between the curved portions of the two bends was approximately $1D$.

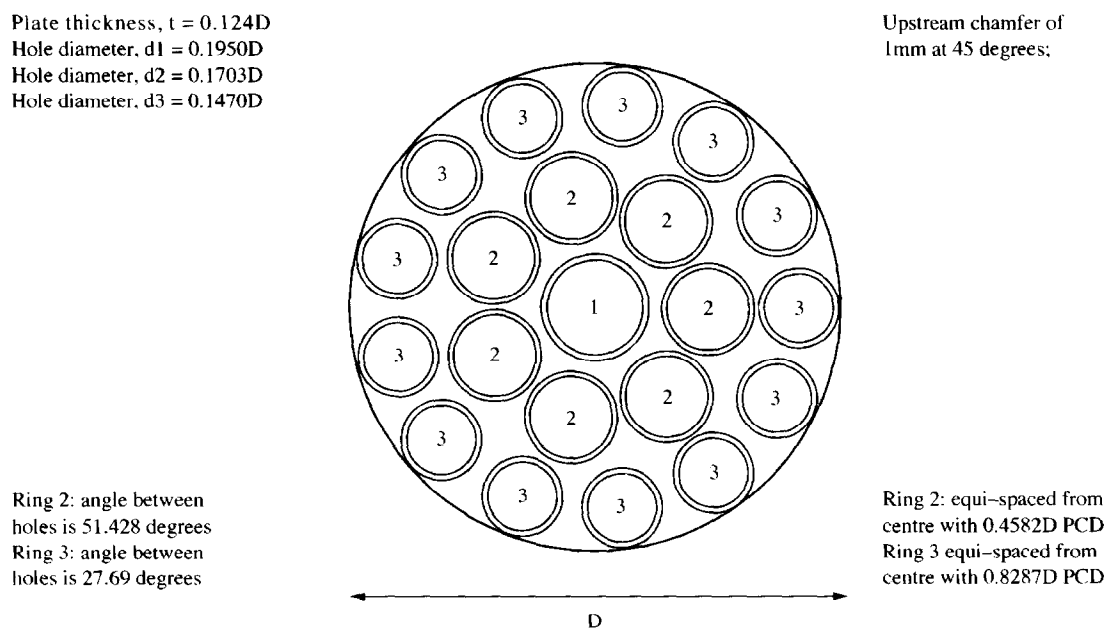
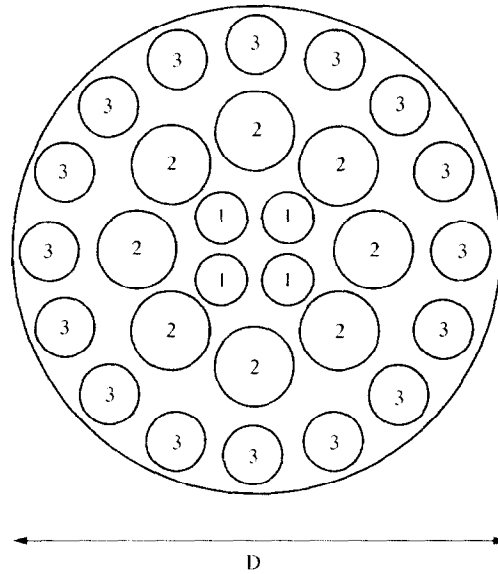


Figure 3 The chamfered Laws flow conditioner

Plate thickness, $t = 0.12D$
 Hole diameter, $d_1 = 0.10D$
 Hole diameter, $d_2 = 0.16D$
 Hole diameter, $d_3 = 0.12D$

Ring 1: angle between holes is 90 degrees
 Ring 2: angle between holes is 45 degrees
 Ring 3: angle between holes is 22.5 degrees



Ring 1: equi-spaced from centre with $0.18D$ PCD
 Ring 2 equi-spaced from centre with $0.48D$ PCD
 Ring 3 equi-spaced from centre with $0.86D$ PCD

Figure 4 The Spearman (NEL) flow conditioner

A schematic of the water test circuit is shown in Figure 5. Prior to reaching the test section, the flow passed through $77D$ of straight pipe, 102.6 mm internal diameter, similar to the test section. This straight length also included an MHI flow conditioner located $27D$ downstream of the nearest flow-disturbing installation which made sure that disturbed flow in the test section originated from the flow-disturbing installations only and not from upstream pipe configurations. The use of a constant head tank eliminated upstream flow pulsations. Downstream of the flow-disturbing installations approximately $48D$ of Perspex pipe (wall thickness 5 mm) was inserted so that laser Doppler velocimetry (LDV) measurements could be made at various

locations downstream of the flow conditioners. The measurement programme was performed with $4D$ between the flow disturbing installations and the flow conditioners. This was installed as one piece of Perspex and the subsequent $44D$ was installed as two pieces to minimise the number of connection flanges and thus the possibility of disturbed flow caused by flange misalignment. Measurements were made on pipe diameters to avoid the requirement for water-filled Perspex boxes. Dantec traverses were used to position the probe volume at the required position. Static pressure was measured at a point $4D$ upstream of the flow-disturbing installations and the test programme was carried out at between 100 and 120 kPa

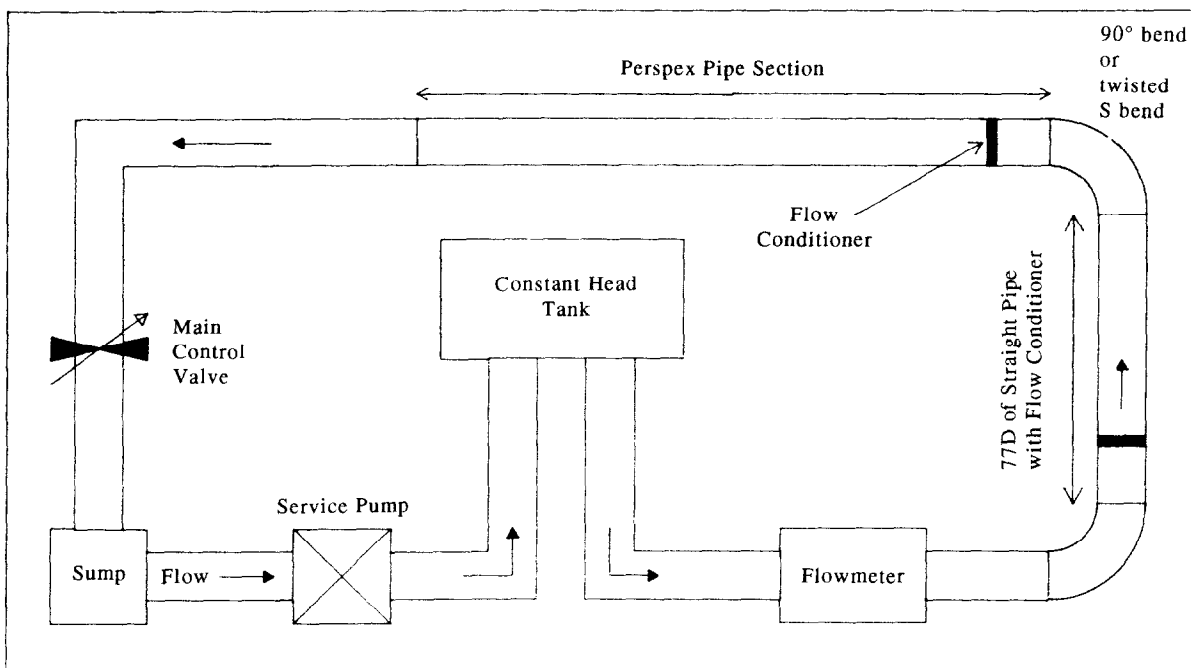


Figure 5 Schematic of the test circuit

above atmospheric pressure. The flowrate throughout the test programme, measured by a turbine meter, was approximately 40 l/s giving rise to Reynolds numbers in the region of 5×10^5 .

Using a one component LDV system, measurements were made of axial velocity (u) and axial root mean square (r.m.s.) fluctuation velocity (u') at various locations downstream of the flow conditioners across two perpendicular diameters (horizontal and vertical). Figure 6 shows the co-ordinate system used for the test programme. Using the measured profiles, comparisons could be made. As yet there are no guidelines on the turbulence profile that is allowable for a flow profile to be considered fully developed. However, the data contained in this paper indicate how the turbulence profile develops downstream of the conditioners and this may help to determine allowable limits of turbulence for orifice plates in the future.

The LDV system used for most of the test programme featured a 15 mW Spectra-Physics He-Ne laser operating in forward scatter at a wavelength of 632.8 nm. A Dantec optical system was used in conjunction with a TSI Intelligent Flow Analyser (IFA) model 550 signal processor and FIND software. Frequency shift was provided by a Dantec frequency shift unit. The probe volume dimensions were approximately $1.0 \times 0.1 \times 0.1$ mm and a Dantec traverse system was used to position the volume within the pipe. A baseline test to determine a fully developed flow profile was also undertaken. This was carried out in the $77D$ of pipe upstream of the flow-disturbing installations. To make sure a fully developed flow profile was present, the measurements were made $43D$ downstream of the unchamfered Laws conditioner (replacing the MHI conditioner owing to the results obtained in the main test programme; the unchamfered Laws conditioner was chosen for its low head loss

coefficient). Unfortunately it was only possible to make a traverse in the horizontal plane. These measurements were made using an air-cooled 100 mW ILT Argon-ion laser operating at a wavelength of 514.5 nm in forward scatter.

Measurements were made at locations of 3, 6, 11, 16, 21, 26, 31, 36 and $41D$ downstream of each installed flow conditioner. These measurements correspond with those made at 7, 10, 15, 20, 25, 30, 35, 40 and $45D$ downstream of the flow-disturbing installations without the insertion of a flow conditioner, and in the latter case additional measurements were also made at $5D$.

4. Results

4.1. Velocity profiles

The velocity profile data have been plotted non-dimensionally with respect to the mean pipe velocity (U) to allow comparison with other data. For each flow conditioner all the data for each measurement plane are plotted for comparison with 5% tolerance limits from the baseline profile, similar to ISO 5167-1 Clause 7.4. The baseline profile, when integrated in accordance with the method of cubics from BS 1042: 2.1 [11], provides an integrated mean pipe velocity that differs from the average mean pipe velocity during the baseline traverse by only 0.17%.

At the pipe wall the measurement uncertainty is increased owing to 'flare', which reduces the signal-to-noise ratio, and the steep velocity gradient which causes any small errors in the positioning of the probe volume to have a more significant effect on the measurement process. Because of this, some points at the pipe wall that fall outside the 5% limits have not been considered as their failure has been judged to be because of the increased measurement uncertainty

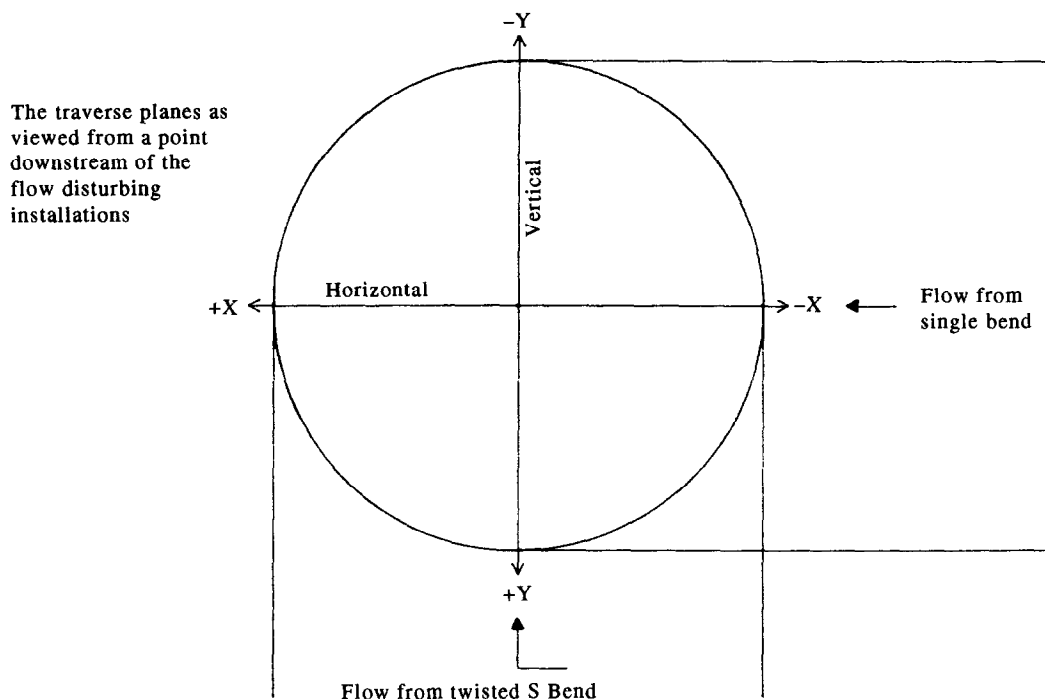


Figure 6 Orientation of the traverse planes

and not because of a particular conditioner's performance. These points will be indicated in the discussion. The maximum uncertainty for all the measurements is approximately 1%.

4.1.1. Single bend.

4.1.1.1. No flow conditioner. The velocity profiles downstream of the single bend without a flow conditioner can be seen in Figures 7 and 8. In the plane of the bend (horizontal plane) it can be seen that the flow profiles only meet the 5% criterion from 35D onwards whereas in the vertical plane the profiles meet the criterion from 30D onwards. This indicates, therefore, that the complete profile only meets the 5% criterion from 35D onwards. The horizontal profiles show that the flow is asymmetrical at 5D in this plane with the highest velocities coinciding with the outside of the bend. The vertical profiles are, as would be expected, more symmetrical at 5D. Both orientations show that the single bend produces a flat profile (the individual points tend to be above the baseline profile near the pipe wall and below the baseline at the centre of the pipe). The flatness decreases with increased distance downstream of the bend.

4.1.1.2. The MHI conditioner. The MHI conditioner produced some interesting results which are shown in Figures 9 and 10. The vertical profiles show an exceptionally consistent result in which the flow profiles are marginally outside the 5% criterion for a few points at 3D downstream of the conditioner but meet the standard from 6D onwards. The horizontal plane however, while showing profiles that meet the 5% criterion between 3 and 11D, also shows that the flow

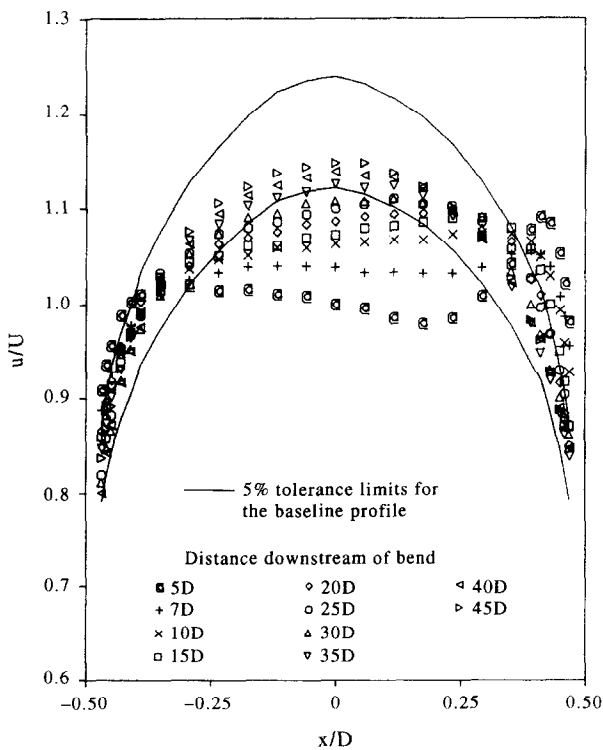


Figure 7 Velocity profiles downstream of the single bend (horizontal plane)

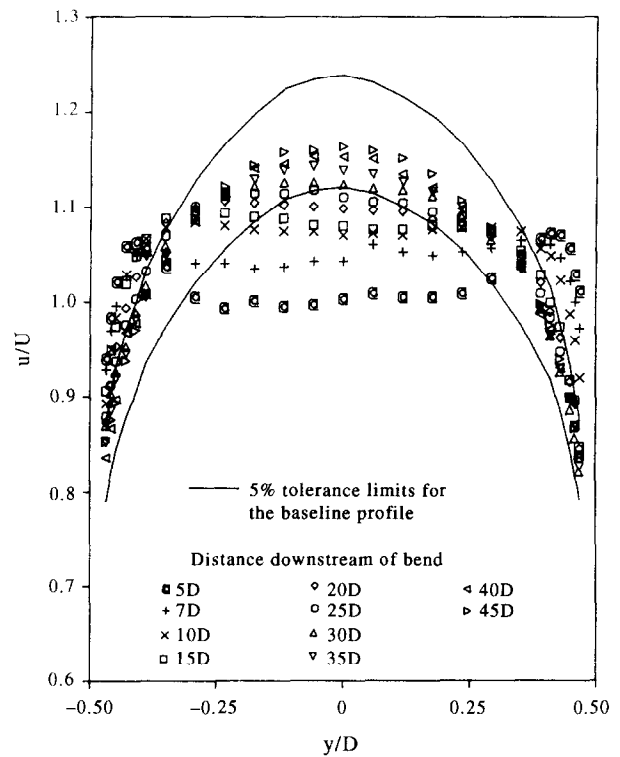


Figure 8 Velocity profiles downstream of the single bend (vertical plane)

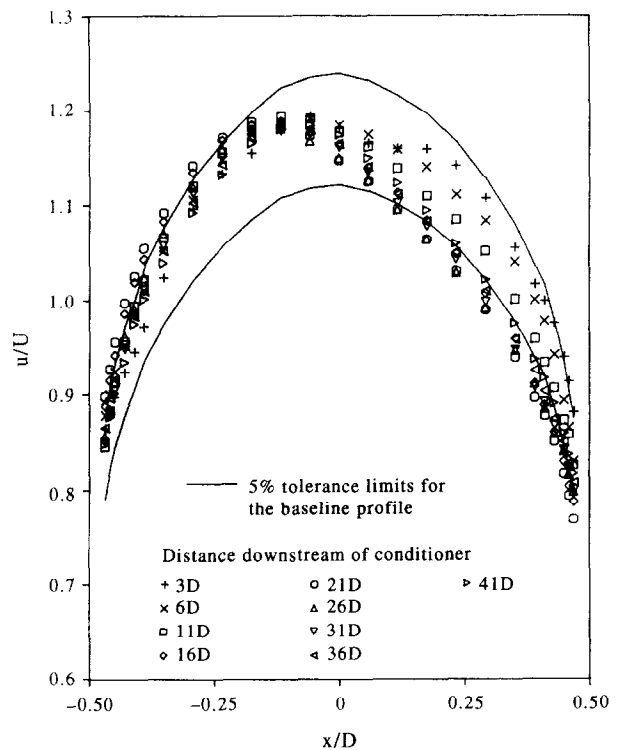


Figure 9 Velocity profiles downstream of the MHI conditioner for the single bend (horizontal plane)

profiles proceed to become asymmetrical from 16D onwards and do not quite meet the 5% criterion even at 41D downstream of the flow conditioner. This asymmetry was first thought to be due to the MHI's lack of rotational symmetry but a repeat profile

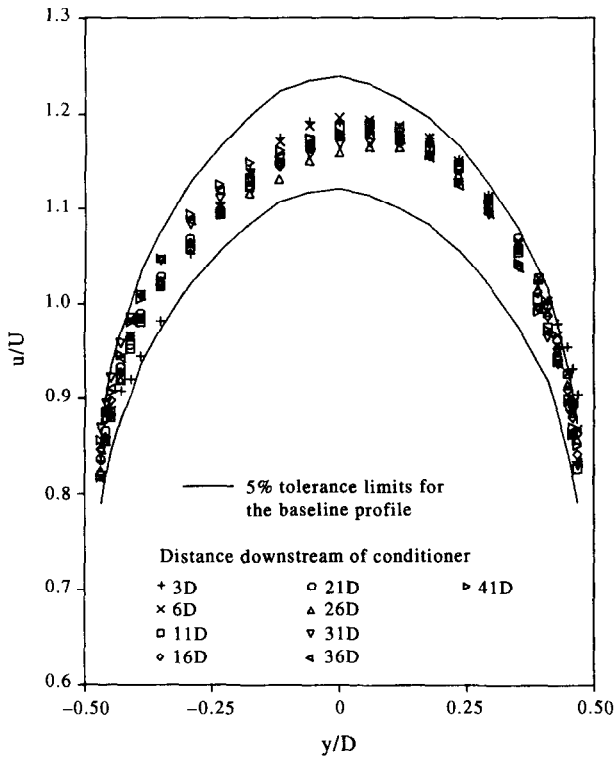


Figure 10 Velocity profiles downstream of the MHI conditioner for the single bend (vertical plane)

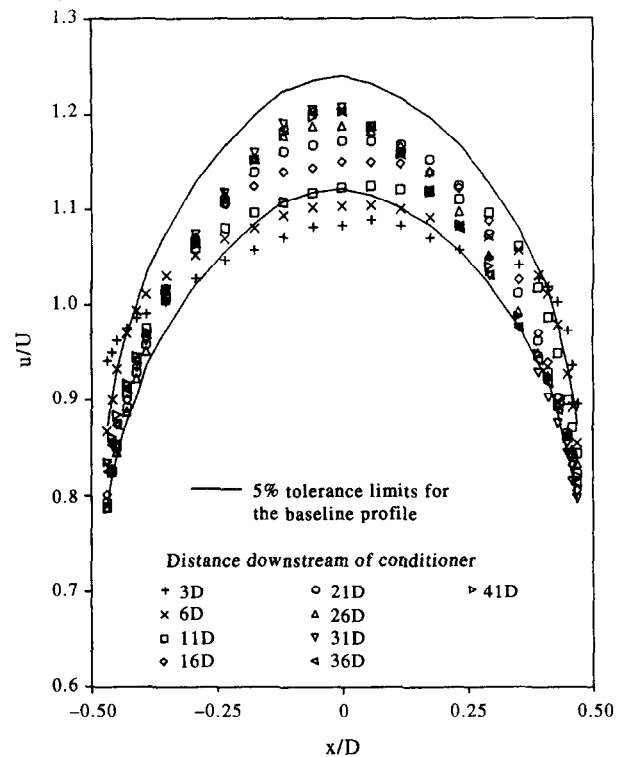


Figure 11 Velocity profiles downstream of the unchamfered Laws conditioner for the single bend (horizontal plane)

obtained after a 90° rotation of the conditioner showed a similar trend. Some researchers have suggested that flow conditioners can actually ‘freeze’ a disturbed profile in certain circumstances but this does not really explain the data obtained in these experiments. Firstly, the asymmetry is in the reverse sense of what would be expected from a frozen profile of the particular bend orientation, and secondly, rather than being frozen, the profiles show definite changes from one location to the next.

4.1.1.3. *The unchamfered Laws conditioner.* The unchamfered Laws flow conditioner produces an entirely different set of profiles which are shown in Figures 11 and 12. Both traverse orientations produce relatively flat profiles initially, although they are an improvement on the no-conditioner case. The horizontal plane data show that the profiles do not meet the standard for distances less than 11D. From 11D onwards, however, the profiles meet the standard apart from at 31D where some points are too low. The vertical data meet the standard from 11D onwards. Both graphs show a large variation in the values at the centre of the pipe.

4.1.1.4. *The chamfered Laws conditioner.* Figures 13 and 14 show the results obtained from the chamfered Laws conditioner. It can be seen that this conditioner is an improvement on the unchamfered version for this installation. The horizontal plane provides data that lie on the 5% criterion at 6D, and from 11D onwards the profiles meet the 5% criterion allowing for a couple of points near the negative pipe wall that appear to fail the criterion probably owing to positioning uncertainty. The vertical plane data meet the criterion from 11D onwards.

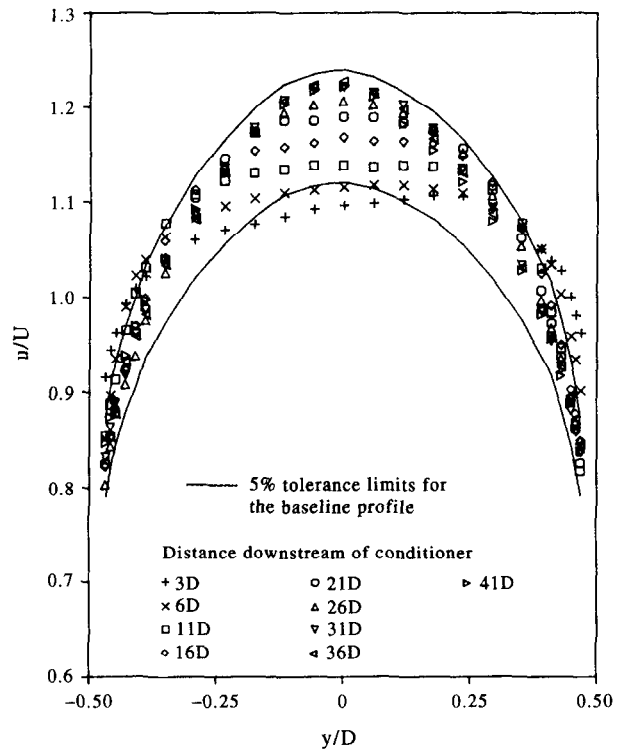


Figure 12 Velocity profiles downstream of the unchamfered Laws conditioner for the single bend (vertical plane)

4.1.1.5. *The Spearman (NEL) conditioner.* Figures 15 and 16 show the data obtained from the Spearman (NEL) conditioner. The profiles in the horizontal plane are interesting in that they are slightly asymmetrical in the same sense as those downstream of the MHI conditioner although the level of asymmetry is signifi-

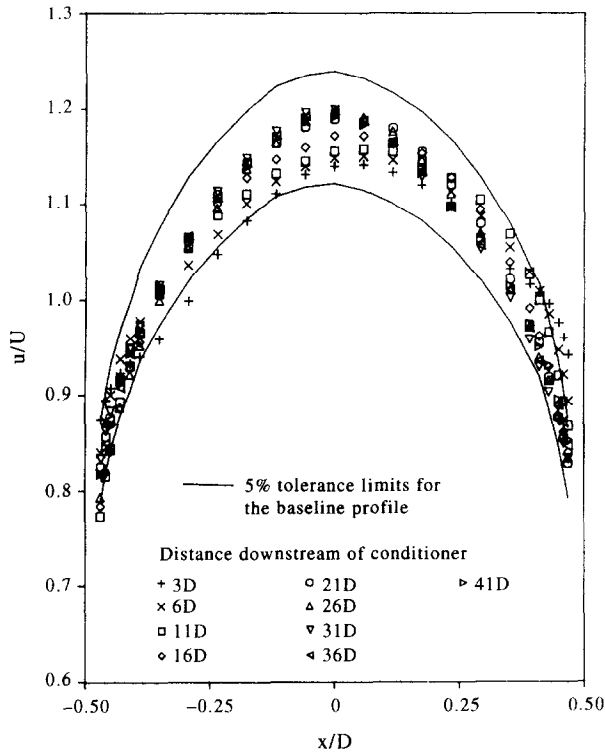


Figure 13 Velocity profiles downstream of the chamfered Laws conditioner for the single bend (horizontal plane)

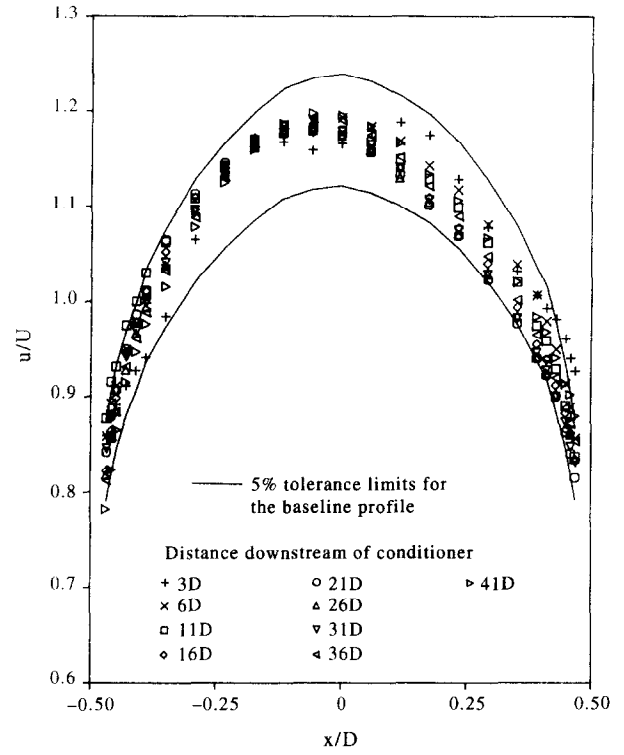


Figure 15 Velocity profiles downstream of the Spearman (NEL) conditioner for the single bend (horizontal plane)

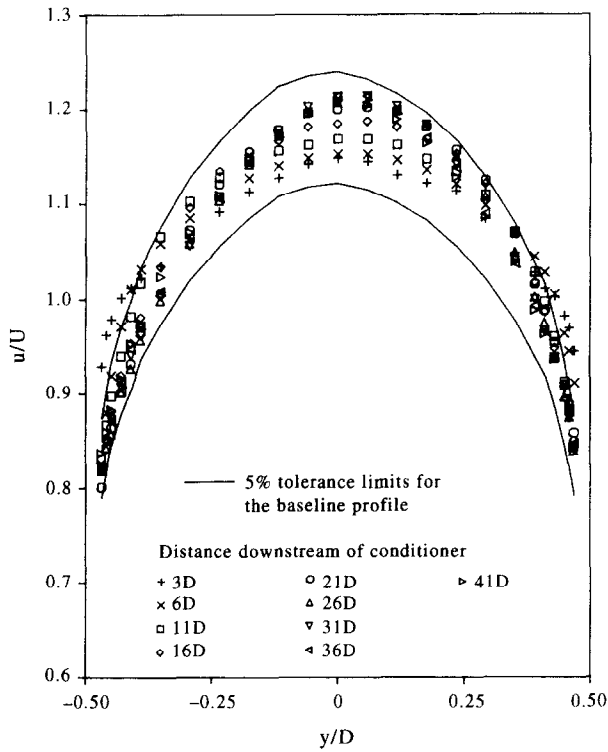


Figure 14 Velocity profiles downstream of the chamfered Laws conditioner for the single bend (vertical plane)

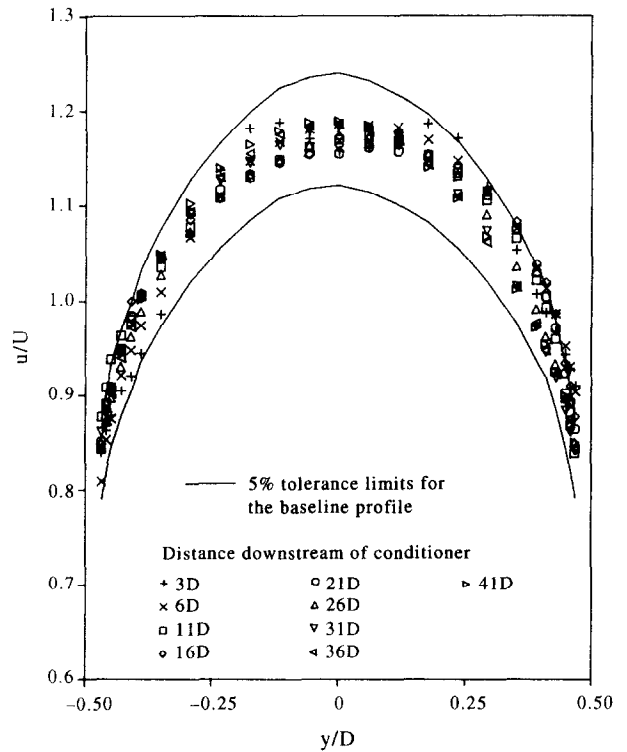


Figure 16 Velocity profiles downstream of the Spearman (NEL) conditioner for the single bend (vertical plane)

cantly less. As a result all the profiles from 6D onwards satisfy the 5% criterion excluding the point at the negative wall for 41D. In the vertical orientation the profiles are more symmetrical, as were those of the MHI conditioner, and the profiles satisfy the 5% criterion from 11D onwards.

4.1.1.6. *Conclusions.* When placed downstream of a single bend most of the flow conditioners improved the flow significantly when compared with the no-conditioner case. The exception appears to be the MHI conditioner, which causes significant downstream asymmetry: while the conditioner appears to produce

good flow conditioning between 6 and 11D, profiles further downstream do not satisfy the 5% criterion to such an extent that it appears that one would be better off not using an MHI conditioner at 31D ($\approx 35D$ downstream of the bend with no flow conditioner). The other conditioners gave satisfactory results from 11D onwards.

4.1.2. Twisted S bend.

4.1.2.1. No flow conditioner. The velocity profiles obtained downstream of the twisted S bend without the insertion of a flow conditioner are asymmetric as shown in Figures 17 and 18. The peak due to the asymmetry slowly corkscrews from one side of the pipe to the other with increasing distance downstream of the installation owing to the swirl present. A relatively flat profile is again obtained, which slowly decays to a fully developed profile, but in the horizontal plane the profiles fail to meet the 5% criterion at 45D. Moreover, one of the important parameters not measured in this test programme is the swirl angle, which must be less than 2° for the profile to be acceptable. The elimination of swirl is very important for orifice plate flowmetering. Tests to measure swirl downstream of conditioners, especially the Spearman (NEL) conditioner, are currently being conducted at NEL. Experiments by Mattingly and Yeh [12] have shown that the swirl angle at 45D downstream of a similar twisted S bend is well in excess of 2° .

4.1.2.2. The MHI conditioner. Figures 19 and 20 show the profiles obtained downstream of the MHI conditioner. The vertical profiles obtained in the plane of the exit bend show some symmetry and the data

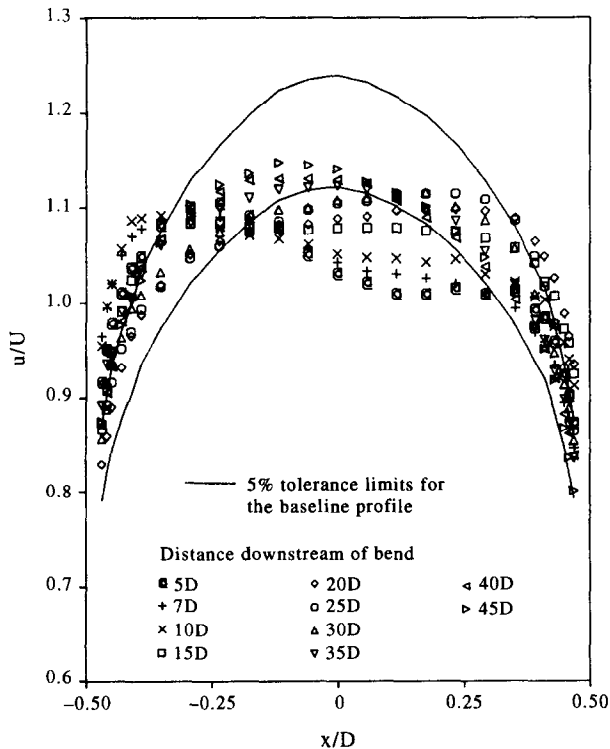


Figure 17 Velocity profiles downstream of the twisted S bend (horizontal plane)

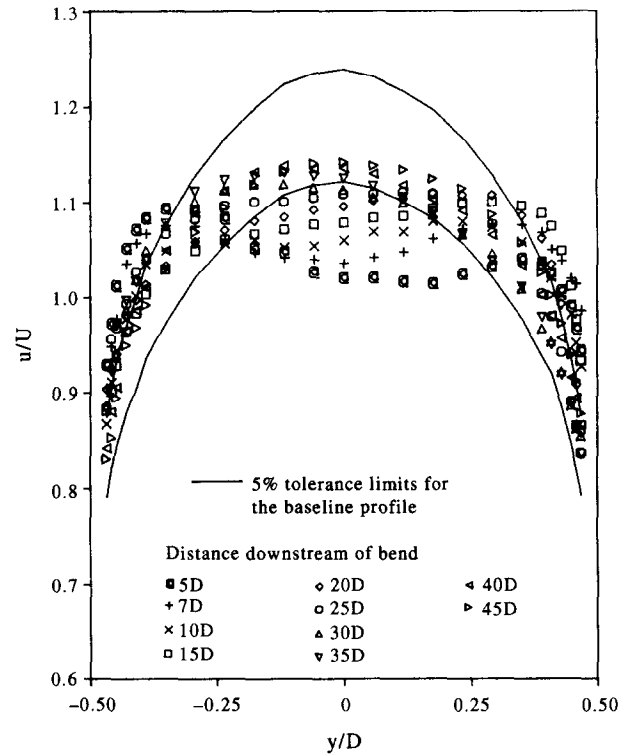


Figure 18 Velocity profiles downstream of the twisted S bend (vertical plane)

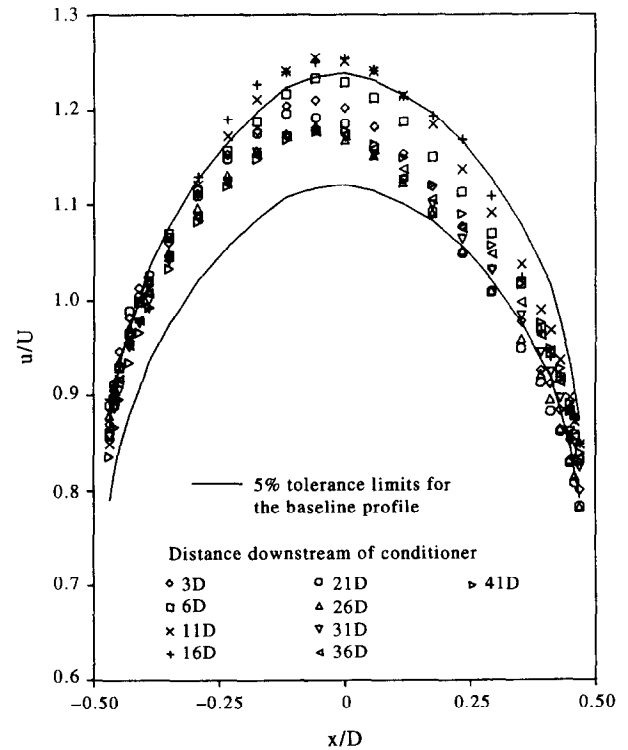


Figure 19 Velocity profiles downstream of the MHI conditioner for the twisted S bend (horizontal plane)

satisfy the 5% criterion from 11D onwards. However, the horizontal orientation shows, as with the single bend, many asymmetrical profiles of which only those from 31D onwards and arguably at 11D satisfy the 5% criterion. This result is consistent with the earlier statement that this conditioner performs better in flows

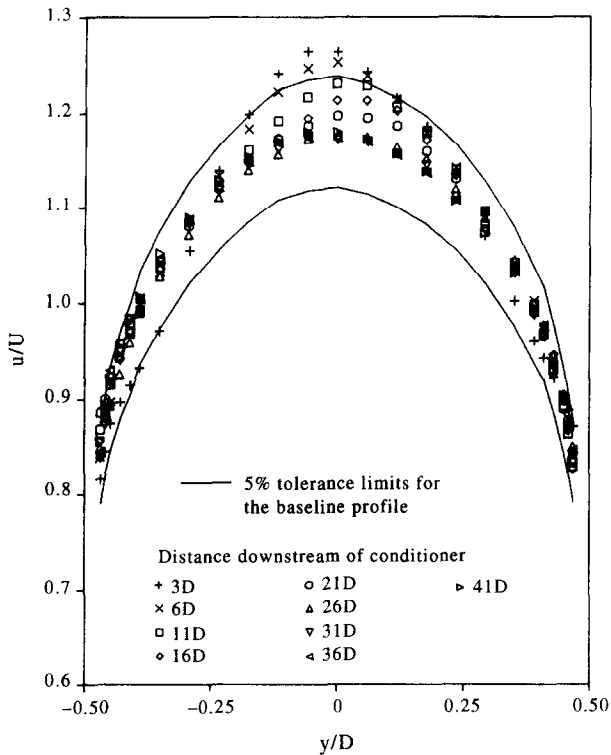


Figure 20 Velocity profiles downstream of the MHI conditioner for the twisted S bend (vertical plane)

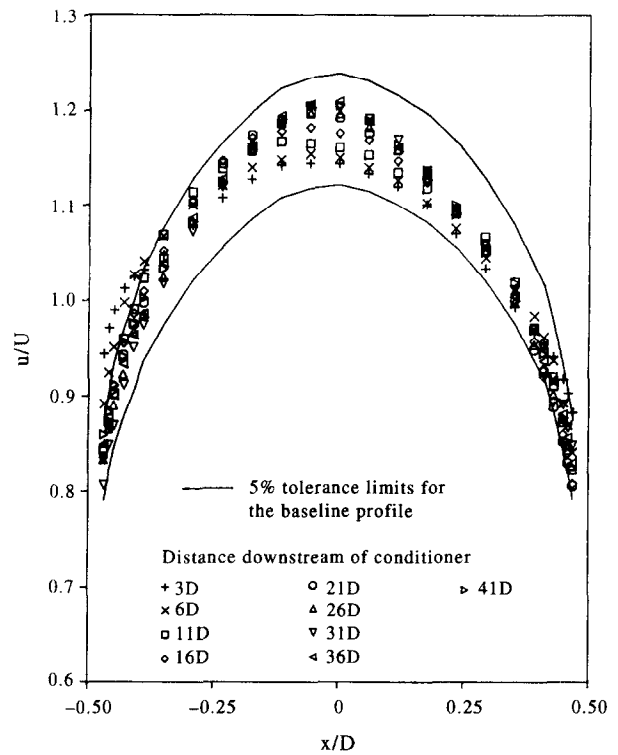


Figure 21 Velocity profiles downstream of the unchamfered Laws conditioner for the twisted S bend (horizontal plane)

with a significant degree of swirl. It is interesting to note that the profiles at the shorter distances are more peaked than those in the single bend case.

4.1.2.3. *The unchamfered Laws conditioner.* The performance of the unchamfered Laws conditioner downstream of the twisted S bend is shown in Figures 21 and 22. Although there is less 'spread' in the values obtained at the centre of the pipe, the profiles are close to failing the criterion at 11D for the vertical plane whereas they passed for the single bend case. The horizontal profiles pass from 11D onwards. It is interesting that the profiles obtained downstream of the twisted S bend are again more peaked than those obtained downstream of the single bend as was the case for the MHI conditioner.

4.1.2.4. *The chamfered Laws conditioner.* Profiles from the chamfered Laws conditioner are shown in Figures 23 and 24. Both sets of profiles show a high degree of symmetry and they also show relatively little spread in the points indicating that the profile approaches a fully developed flow profile very quickly. The data from the horizontal plane pass from 6D onwards whereas the vertical plane data satisfy the 5% criterion from 11D onwards. Although the actual distance required downstream of the conditioner to satisfy the 5% criterion is essentially the same, the profiles obtained downstream of the twisted S bend are better than those obtained downstream of the single bend in that the spread of the points is much reduced for the twisted S bend case.

4.1.2.5. *The Spearman (NEL) conditioner.* The profiles obtained downstream of the Spearman (NEL) con-

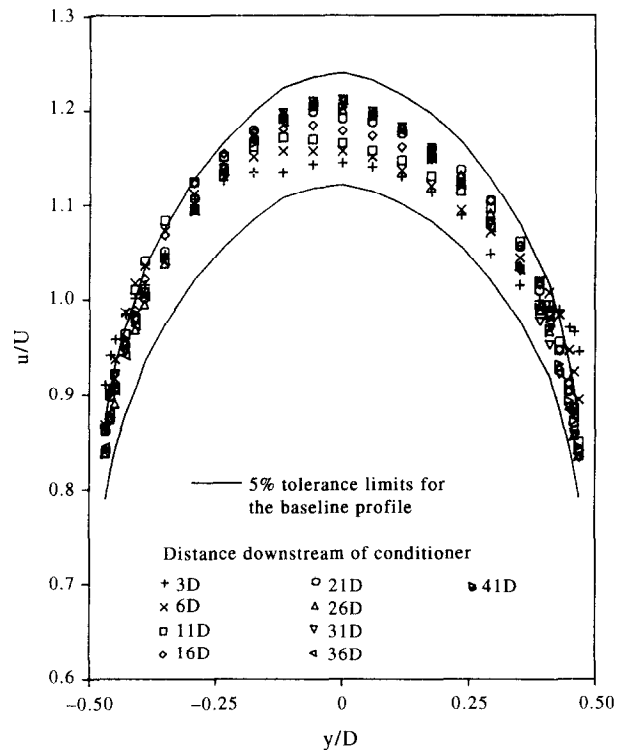


Figure 22 Velocity profiles downstream of the unchamfered Laws conditioner for the twisted S bend (vertical plane)

ditioner are shown in Figures 25 and 26. If the 5% criterion is applied the profiles from this flow conditioner in the horizontal orientation are satisfactory from 6D onwards although the 26D profile has one point that just fails. The vertical plane satisfies the criterion from 6D onwards also, and so this conditioner shows

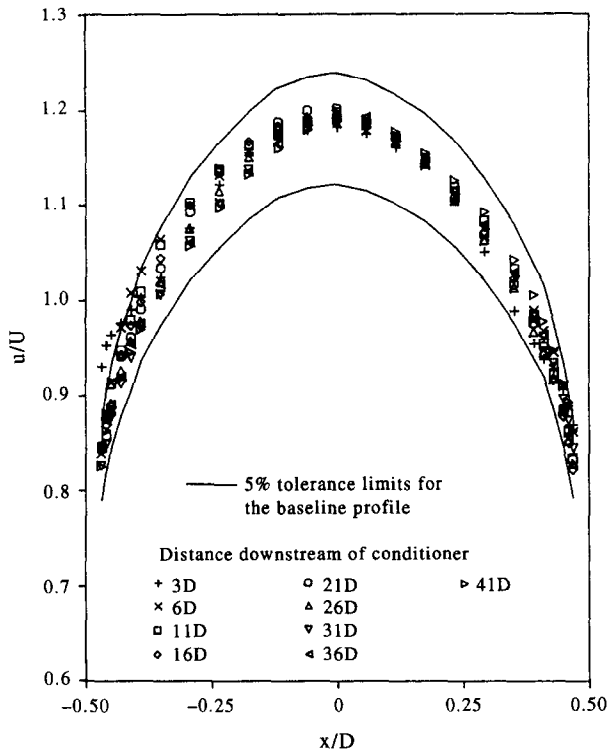


Figure 23 Velocity profiles downstream of the chamfered Laws conditioner for the twisted S bend (horizontal plane)

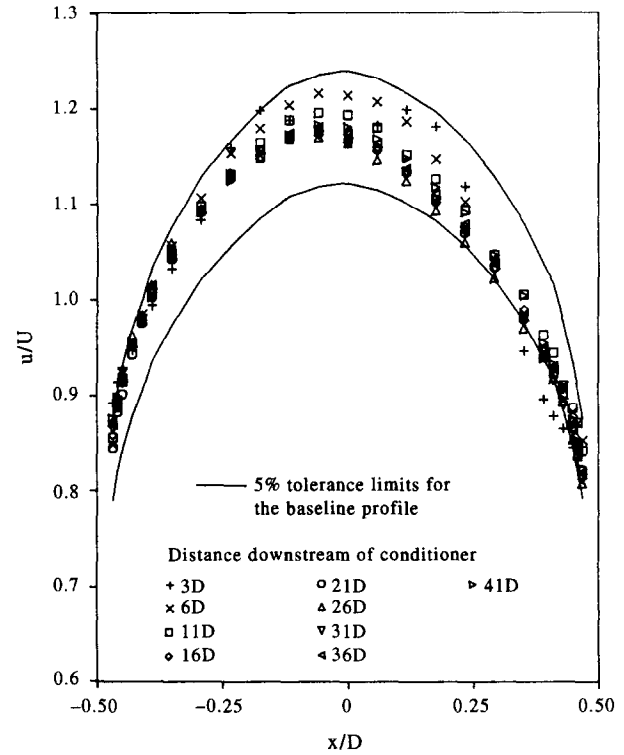


Figure 25 Velocity profiles downstream of the Spearman (NEL) conditioner for the twisted S bend (horizontal plane)

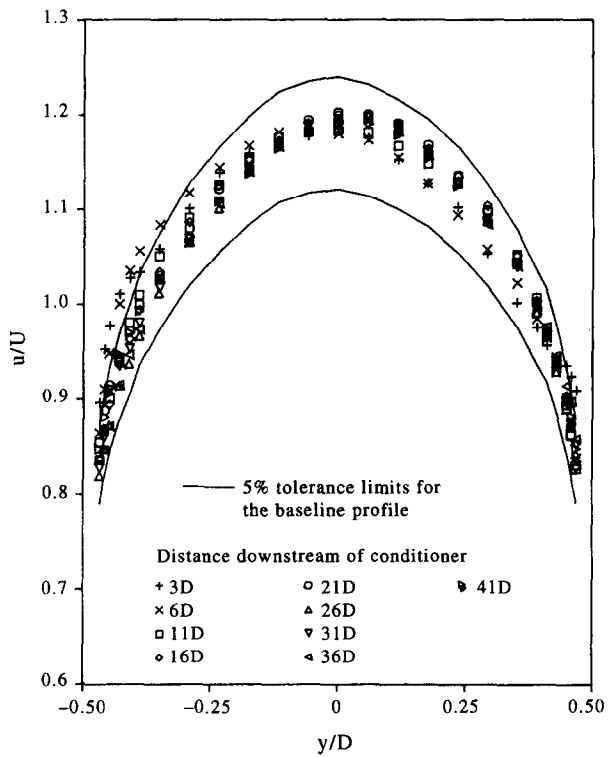


Figure 24 Velocity profiles downstream of the chamfered Laws conditioner for the twisted S bend (vertical plane)

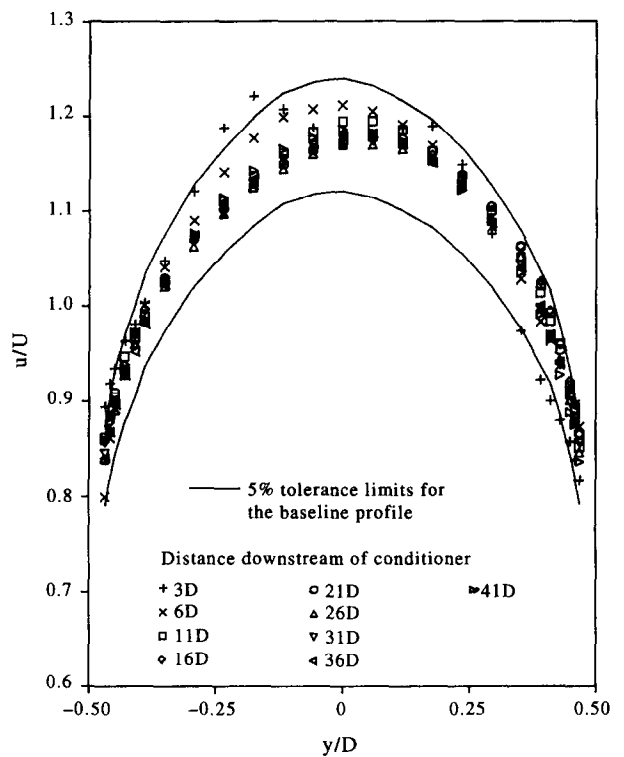


Figure 26 Velocity profiles downstream of the Spearman (NEL) conditioner for the twisted S bend (vertical plane)

a marked improvement from its performance for the single bend case.

4.1.2.6. *Conclusions.* As was the case for the single bend, the MHI conditioner appears to be the least successful in that it requires a significant downstream

distance before the profiles satisfy the 5% criterion. It appears that a more peaked profile is obtained immediately downstream of some of the conditioners compared with the single bend case. Of the conditioners tested it appears that on the basis of the 5% criterion, the Spearman (NEL) conditioner performed

best under these conditions as it passes from $6D$ onwards.

4.2. Turbulence profiles

Unlike the effect of axial velocity profile, the effect of turbulence upon the accuracy of orifice plate flowmeters is far less well understood. Recently Karnik [13, 14] has made measurements using tube bundles and has shown that a flow with a nearly fully developed velocity profile but with a turbulence profile of less magnitude than that obtained in developed flow produces larger discharge coefficients for orifice plates than would otherwise be expected. Likewise a turbulence profile greater in magnitude than that obtained in ideal flow conditions produces lower discharge coefficients. It was also shown that orifice plates returned similar discharge coefficients to those expected in developed flow when located in flow conditions where the magnitude of the turbulence profile was far less than that obtained in developed flow whereas the velocity profile was flat (which is a well known cause of low discharge coefficients). It was concluded that the turbulence had 'cancelled out' the effect of the velocity profile, a conclusion also suggested by Lake and Reid [10].

In conjunction with velocity profile measurements therefore, measurements were also made of the r.m.s. fluctuation velocity (u') to observe how turbulence develops downstream of the two flow-disturbing installations and to assess what, if any, differences there are in the way turbulence develops downstream of the flow conditioners. As was the case with the velocity data, a baseline was measured in fully developed flow conditions to provide a reference against which all the subsequent profiles could be measured. If compared with the measurements of Karnik and Laufer [15], the baseline agrees reasonably well but does indicate slightly higher turbulence near the pipe wall. For instance Laufer's turbulence data are roughly $u'/U=0.03$ at the centre of the pipe rising to approximately 0.075 close to the pipe wall as opposed to 0.035 and 0.09 for the NEL baseline. Karnik's data are similar to the NEL baseline at the centre of the pipe but resemble Laufer's data nearer the pipe wall. As with the velocity data, all graphs have been non-dimensionalised with respect to the mean pipe velocity.

4.2.1. Single bend.

4.2.1.1. No flow conditioner. The r.m.s. fluctuation velocity profiles obtained downstream of the single bend are shown in Figures 27 and 28. Both horizontal and vertical profiles show that at short distances downstream of the bend the r.m.s. fluctuation velocity is increased significantly compared with the baseline. This turbulence decreases with further distance downstream of the bend but both figures show a significant amount of asymmetry also. The figures show that at $45D$ downstream of the bend the r.m.s. profile is still noticeably different from the baseline profile especially at the centre of the pipe, where the profile, while reasonably symmetrical, is still above that of the baseline.

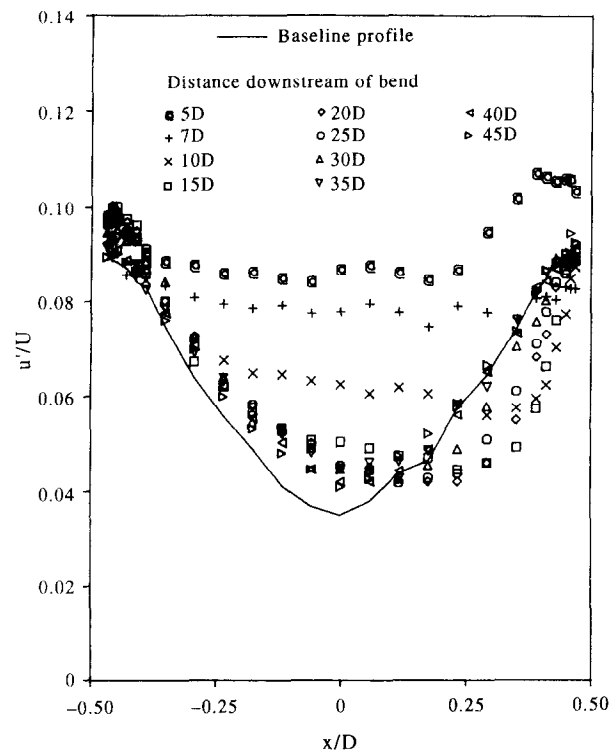


Figure 27 r.m.s. Profiles downstream of the single bend (horizontal plane)

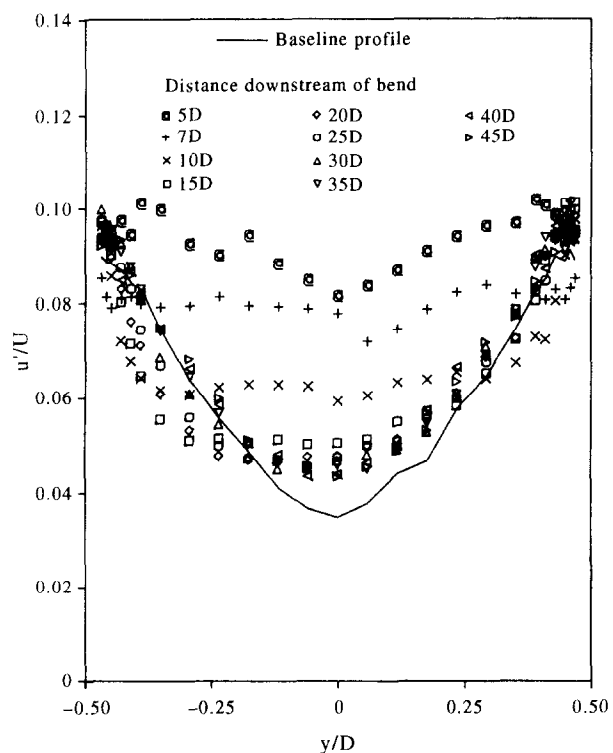


Figure 28 r.m.s. Profiles downstream of the single bend (vertical plane)

4.2.1.2. The MHI conditioner. Figures 29 and 30 show the profiles obtained downstream of the MHI conditioner. The most noticeable difference between these figures and the previous two is that the spread of data is greatly reduced indicating that the MHI conditioner is effective at reducing the turbulence

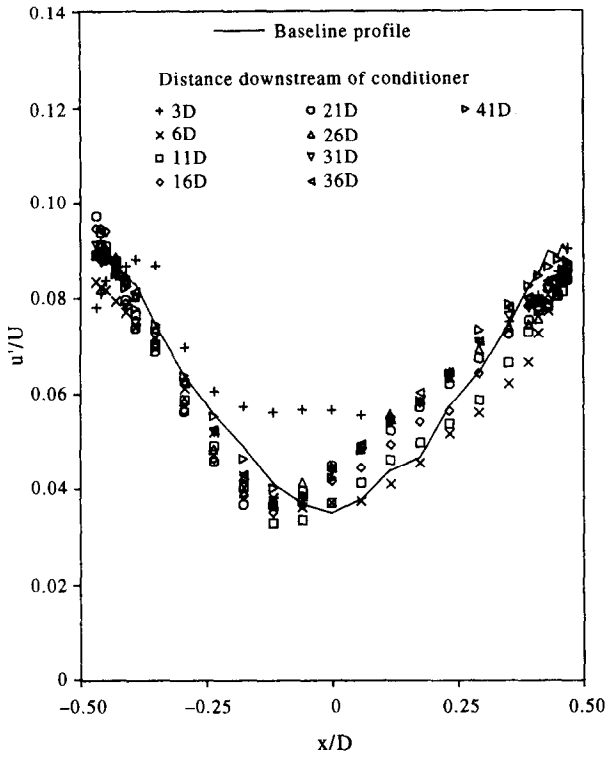


Figure 29 r.m.s. Profiles downstream of the MHI conditioner for the single bend (horizontal plane)

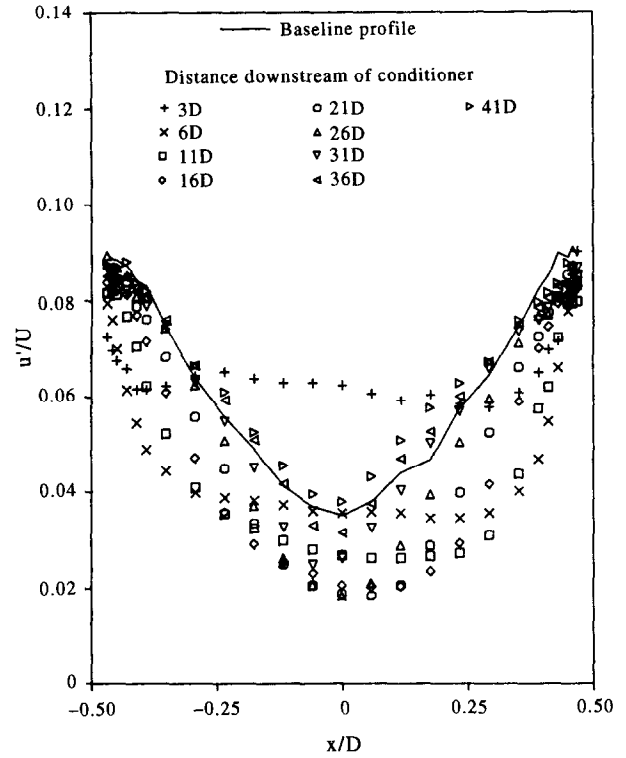


Figure 31 r.m.s. Profiles downstream of the unchamfered Laws conditioner for the single bend (horizontal planes)

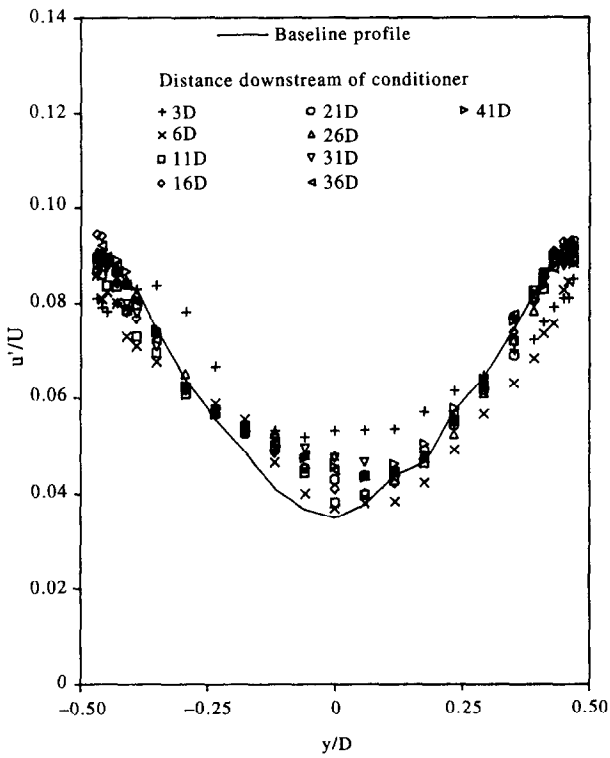


Figure 30 r.m.s. Profiles downstream of the MHI conditioner for the single bend (vertical plane)

within a short downstream distance. Once reduced, the r.m.s. profile alters relatively little with increasing downstream distance and both figures show that the spread for each traverse point is generally no more than 0.01 from 11D onwards. However, the drawback, as was the case for the velocity profiles, is that the

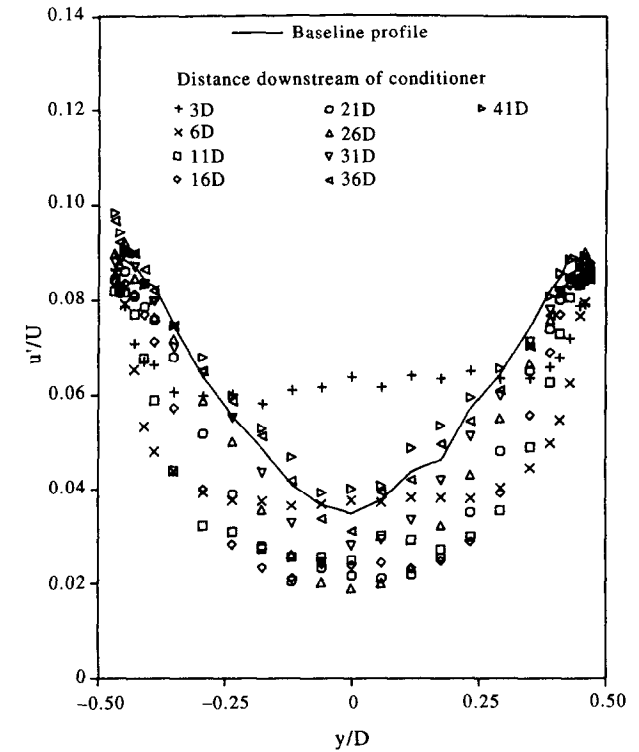


Figure 32 r.m.s. Profiles downstream of the unchamfered Laws conditioner for the single bend (vertical plane)

conditioner has produced significantly asymmetric profiles especially in the horizontal plane which continue to be present at 41D downstream of the conditioner.

4.2.1.3. *The unchamfered Laws conditioner.* In many ways the profiles obtained from the unchamfered Laws conditioner are very different (Figures 31 and 32). This

time there is a greater spread to the data, particularly at the centre of the pipe. The data generally lie below the baseline profile indicating that orifice plate coefficients would be greater than they would normally be in developed flow in the absence of any velocity profile effect. Indeed, the profile of least turbulence appears to be obtained at 26D downstream of the conditioner where the value at the centre of the pipe is roughly half that of the baseline profile for both planes. For distances less than 26D, the turbulence reduces in general with increasing distance from the conditioner and it increases for distances greater than 26D. It is interesting to note that in contrast to the MHI profiles which were relatively V-shaped from 6D onwards, the unchamfered Laws profiles are initially U-shaped. A small amount of asymmetry is shown in these profiles.

4.2.1.4. *The chamfered Laws conditioner.* The chamfered Laws conditioner appears to improve slightly on the unchamfered version in that the amount of spread in the data has been significantly reduced (Figures 33 and 34). However, much of the data continue to lie below the baseline profile and it can be seen that the r.m.s. fluctuation velocity reaches a minimum at 21D downstream of the conditioner as opposed to 26D for the unchamfered version. The magnitude of r.m.s. fluctuation velocity at the centreline at 21D is roughly two thirds that of the baseline profile. This would tend to cause higher orifice plate discharge coefficients (disregarding any velocity profile effects). Like the unchamfered version, a small amount of asymmetry is shown in these profiles.

4.2.1.5. *The Spearman (NEL) conditioner.* The Spearman (NEL) conditioner data (Figures 35 and 36) appear

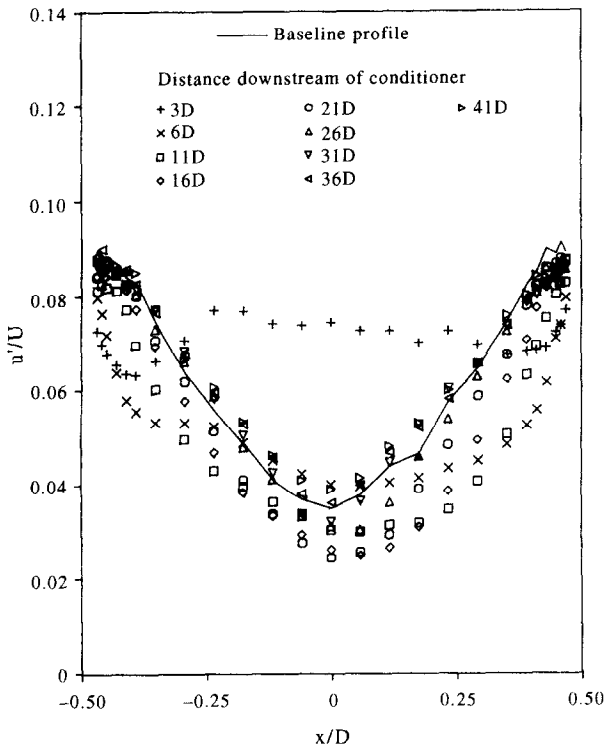


Figure 33 r.m.s. Profiles downstream of the chamfered Laws conditioner for the single bend (horizontal plane)

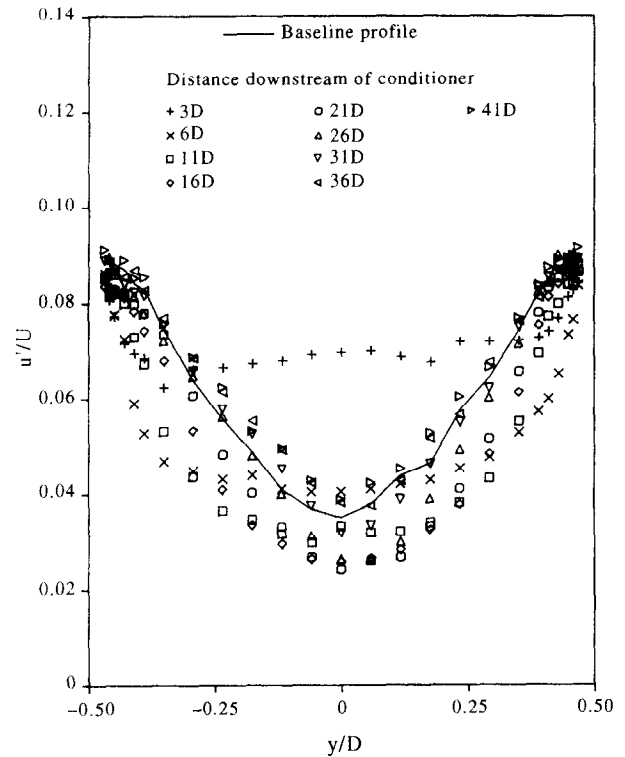


Figure 34 r.m.s. Profiles downstream of the chamfered Laws conditioner for the single bend (vertical plane)

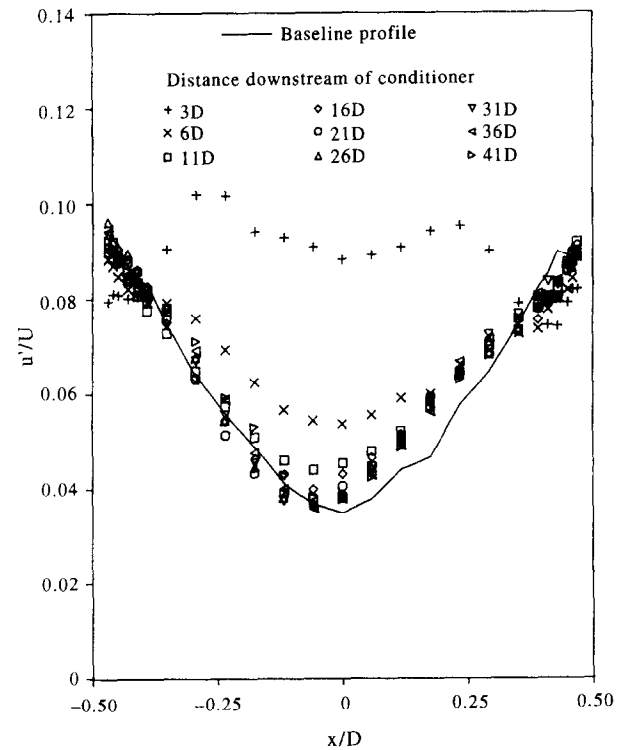


Figure 35 r.m.s. Profiles downstream of the Spearman (NEL) conditioner for the single bend (horizontal plane)

to have more in common with those from the MHI conditioner than those from the Laws conditioners. There is less spread to the data, and unlike the Laws conditioners where the r.m.s. profiles reduce to a minimum level (which is far less than the baseline profile) at around 21D to 26D, the r.m.s. profiles, at

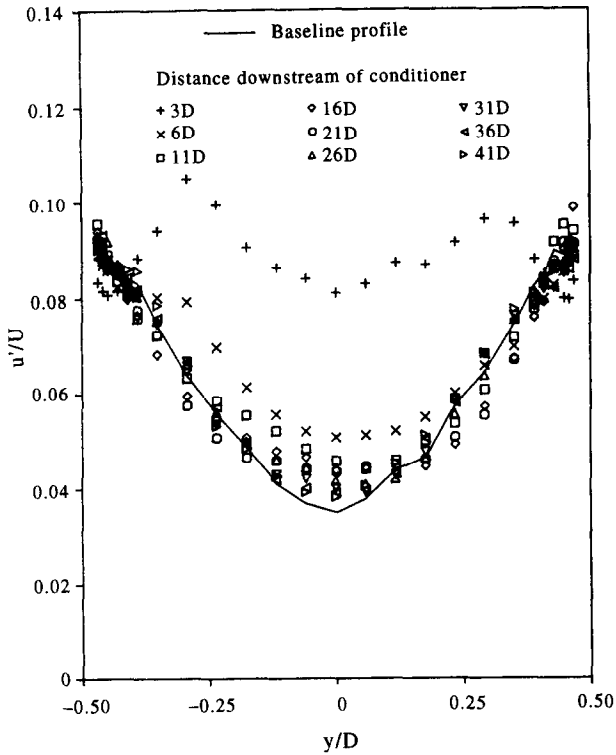


Figure 36 r.m.s. Profiles downstream of the Spearman (NEL) conditioner for the single bend (vertical plane)

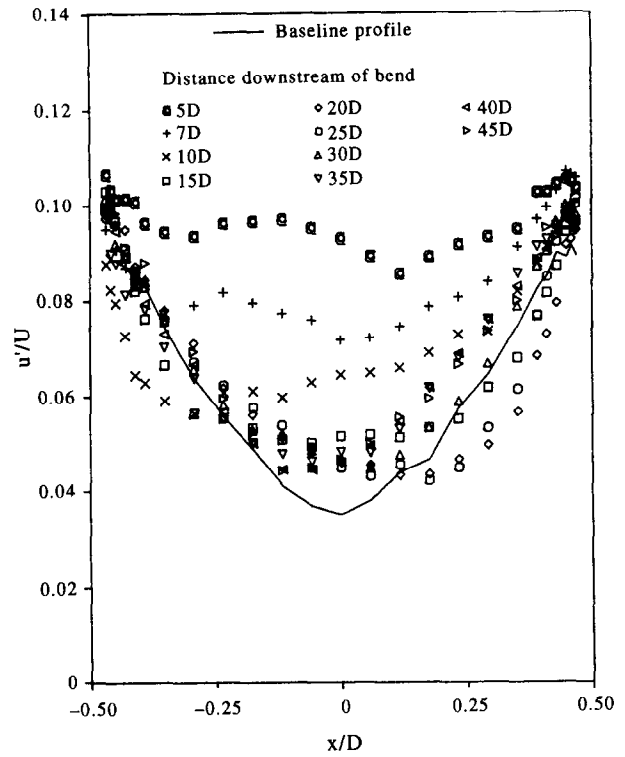


Figure 37 r.m.s. Profiles downstream of the twisted S bend (horizontal plane)

least at the centreline, reduce towards the level of the baseline without any cross-over. As a result, therefore, the data lie above the baseline which, according to the theory, would tend to cause lower discharge coefficients (again disregarding any velocity profile effects); at the acceptable velocity profile distance of 11D the turbulence profile is noticeably above the baseline. There is a small amount of asymmetry in the profiles.

4.2.2. Twisted S bend.

4.2.2.1. No flow conditioner. Figures 37 and 38 show the r.m.s. fluctuation velocity profiles obtained downstream of the twisted S bend. As was the case with the single bend, the twisted S bend has, in general, increased the turbulence significantly with respect to the baseline although profile asymmetry causes some data to lie below the baseline. It is interesting to note that at the centreline both graphs show very little spread in the data from 15D onwards while at, for instance, x and $y/D = \pm 0.25$ the spread is up to four times greater. This is because the twisted S bend produces a swirling flow with asymmetry resulting in a turbulence flow profile where the trough, usually located at the centre of the pipe, corkscrews from one side of the pipe to the other as the asymmetrical flow travels down the pipe with the pipe centreline approximately the axis of this oscillation. The r.m.s. profile at 45D downstream of the bend is still significantly different from the baseline profile.

4.2.2.2. The MHI conditioner. Figures 39 and 40 show the profiles obtained downstream of the MHI conditioner. Again, the profiles show a significant reduction in turbulence with relatively little spread in

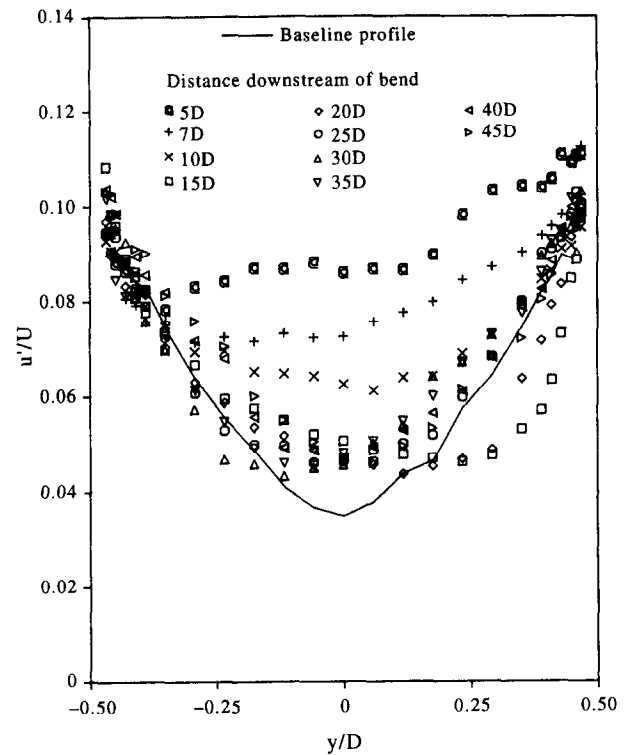


Figure 38 r.m.s. Profiles downstream of the twisted S bend (vertical plane)

the data although there is some asymmetry in some of the profiles. The data generally lie above the baseline especially at the centre of the pipe which suggests that the discharge coefficient of an orifice plate located in these profiles would be lower than if it had been located in fully developed flow conditions

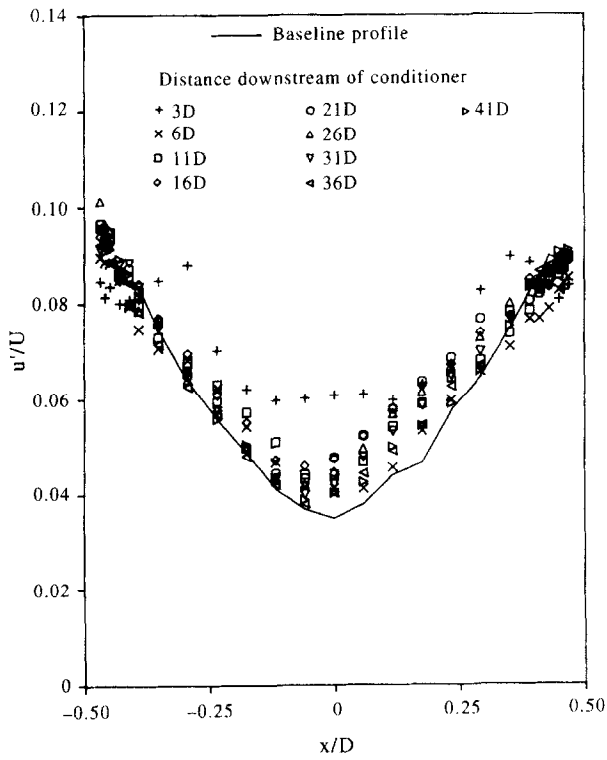


Figure 39 r.m.s. Profiles downstream of the MHI conditioner for the twisted S bend (horizontal plane)

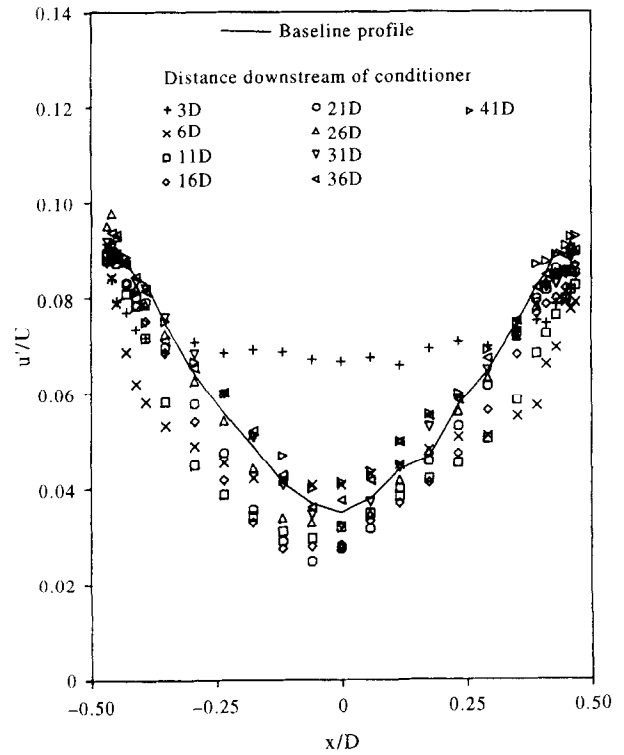


Figure 41 r.m.s. Profiles downstream of the unchamfered Laws conditioner for the twisted S bend (horizontal plane)

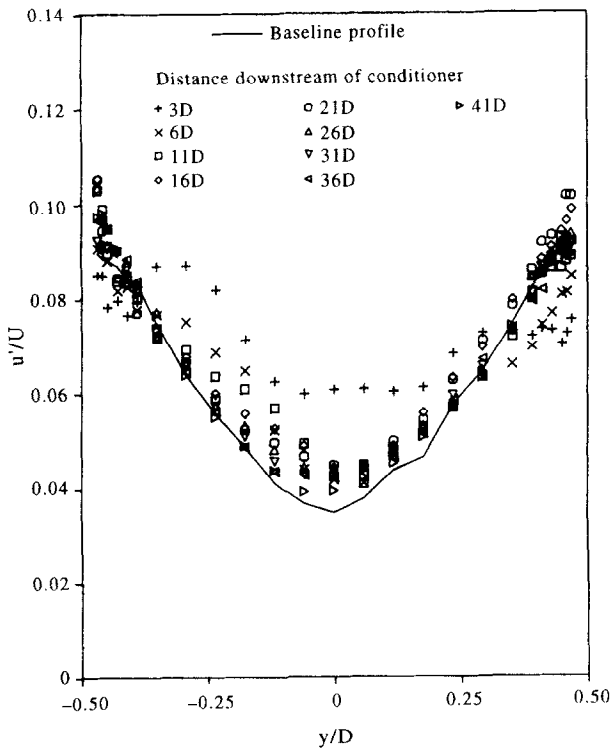


Figure 40 r.m.s. Profiles downstream of the MHI conditioner for the twisted S bend (vertical plane)

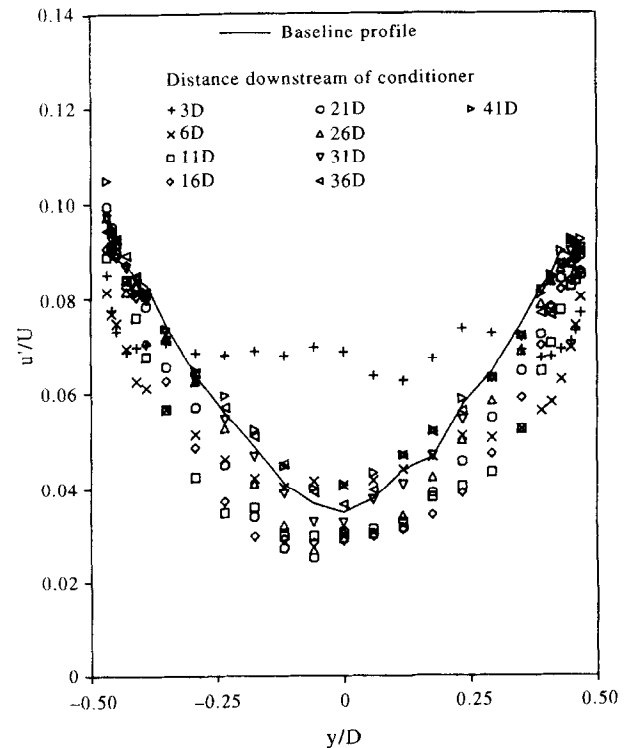


Figure 42 r.m.s. Profiles downstream of the unchamfered Laws conditioner for the twisted S bend (vertical plane)

(disregarding velocity profile effects). However, at 41D downstream of the conditioner both planes show profiles that would be very close to the baseline profile had it not been for the asymmetry.

4.2.2.3. The unchamfered Laws conditioner. Figures 41 and 42 show the r.m.s. fluctuation velocity profiles obtained downstream of the unchamfered Laws conditioner. In comparison with its performance downstream of the single bend there has been a reduction in the amount of spread present in the data although

there does appear to be slightly more asymmetry. As was the case previously, most of the data lie below the baseline which would tend to produce high discharge coefficients (disregarding velocity profile effects). Because of the asymmetry it is more difficult to specify the downstream distance where the r.m.s. fluctuation velocity is at a minimum. However, for both planes 21D appears to be the distance at which the r.m.s. fluctuation velocity is at a minimum at the centreline.

4.2.2.4. *The chamfered Laws conditioner.* The chamfered version (Figures 43 and 44) also produces profiles that have less spread than in the corresponding single bend case and they also show quite a high level of symmetry. The profiles also show a reduction in r.m.s. fluctuation velocity to a minimum at between 16D and 21D. At 11D at which the velocity profile is acceptable, the data near the centreline are very close to the baseline in the horizontal plane and lie on the baseline in the vertical plane.

4.2.2.5. *The Spearman (NEL) conditioner.* The Spearman (NEL) conditioner (Figures 45 and 46) produces r.m.s. fluctuation velocity profiles very similar to those obtained with this conditioner downstream of the single bend especially in the horizontal plane. This would indicate, therefore, that the conditioner is relatively installation independent with respect to r.m.s. fluctuation velocity at least for these two flow-disturbing installations. However, the conditioner still produces profiles above the baseline which are also slightly asymmetric. The data tend to reach a final equilibrium much faster than those with the Laws conditioners, and for both planes there is almost no difference in the data for 26D and beyond.

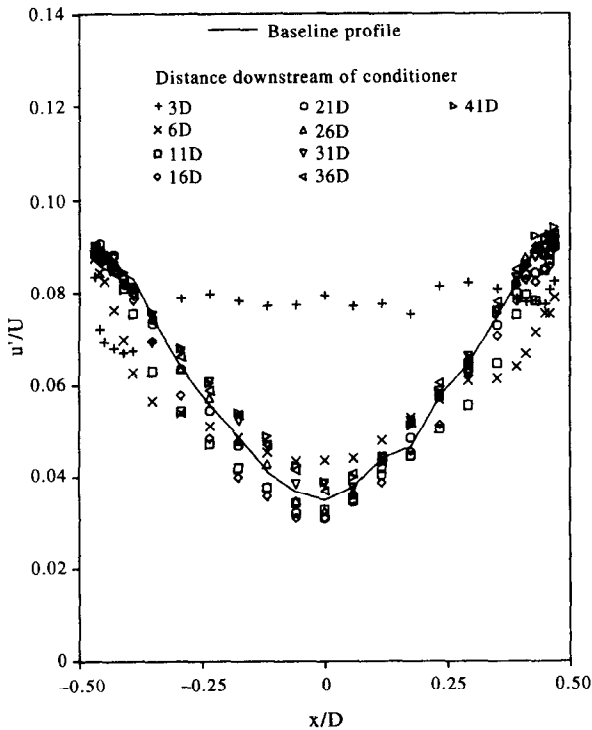


Figure 43 r.m.s. Profiles downstream of the chamfered Laws conditioner for the twisted S bend (horizontal plane)

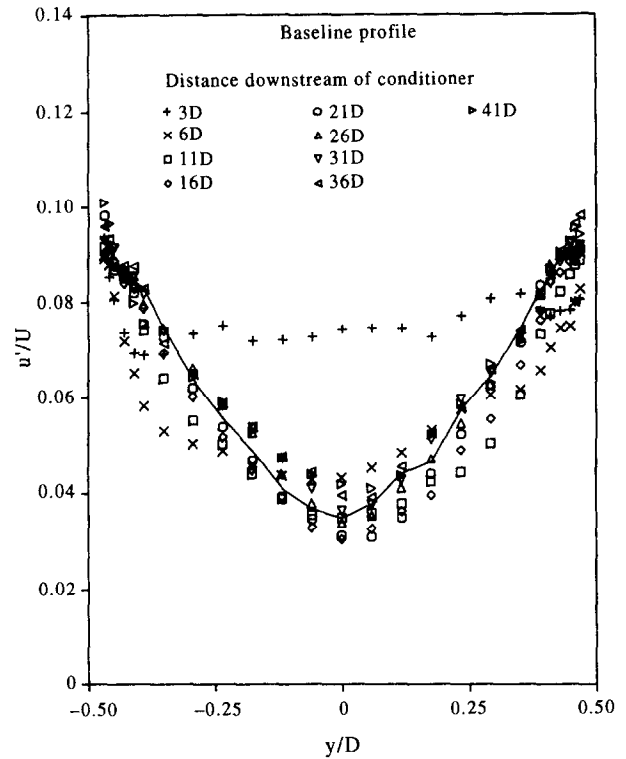


Figure 44 r.m.s. Profiles downstream of the chamfered Laws conditioner for the twisted S bend (vertical plane)

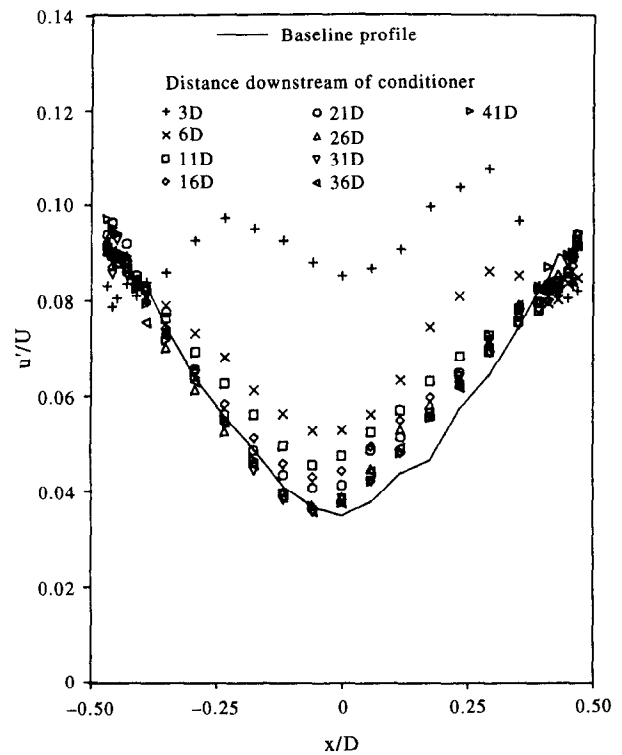


Figure 45 r.m.s. Profiles downstream of the Spearman (NEL) conditioner for the twisted S bend (horizontal plane)

4.2.2.6. *Conclusions.* In contrast to its performance with respect to the velocity profile, the MHI conditioner was very successful at reducing the r.m.s. fluctuation velocity caused by the flow-disturbing installations although it still reflected the asymmetry

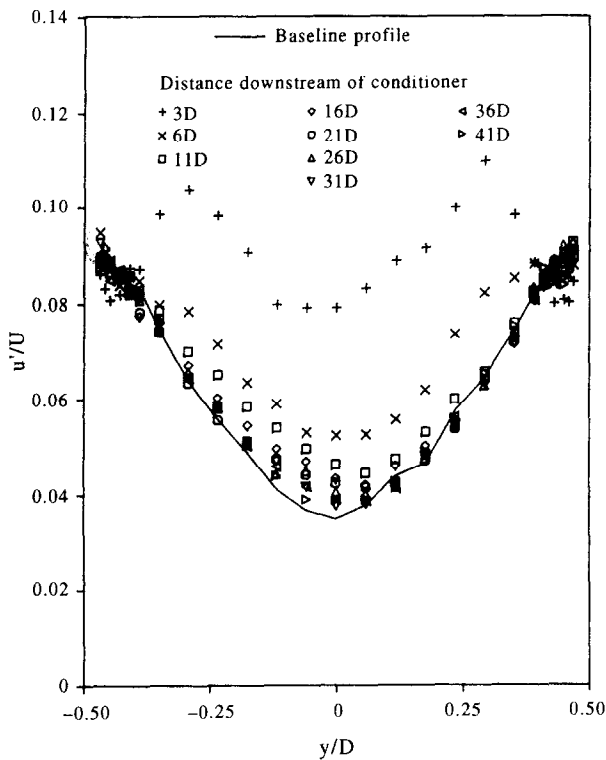


Figure 46 *r.m.s.* Profiles downstream of the Spearman (NEL) conditioner for the twisted S bend (vertical plane)

apparent in the velocity profiles. The Laws conditioners tended to reduce the *r.m.s.* fluctuation velocity too much, especially downstream of the single bend. Better results were obtained for the twisted S bend than the single bend. The Spearman (NEL) conditioner produced very similar profiles for both installations. However, the *r.m.s.* fluctuation velocity is not reduced as quickly as was the case for the MHI conditioner. It is possible that this could be improved by the application of a chamfer to the holes on the upstream face of the conditioner and there are plans to test such a variation in the near future. It is interesting to note that downstream of all the conditioners the spread of the data at the pipe walls is relatively small compared with the spread in the centre of the pipe.

5. Measurements to determine head loss coefficient

Measurements were made of differential pressure across the conditioners to determine the head loss coefficient (K). These measurements are important for two reasons. Firstly, the pressure drop across a flow conditioner (or any other component) is a key factor for closed conduits. If the flow is being pumped, additional energy will be required to overcome the pressure drop. Moreover, conditioners with a high loss coefficient could cause sufficient pressure loss in the pipework to produce cavitation. However, some pressure loss is necessary to condition asymmetrical flow. Measurements were made in NEL's large water flow facility. The differential pressure was measured using two pairs of diametrically opposed tapings: one pair positioned $2D$ upstream of the flow conditioner and the other pair placed $6D$ downstream of the flow

conditioner. The pressure tapings were connected to a manometer. The head loss coefficient is defined as follows:

$$\Delta P = K(1/2\rho U^2) \quad (1)$$

where ΔP is the differential pressure, U is the mean pipe velocity determined from NEL's gravimetric system and ρ is the density of the water. Values of ΔP were obtained at various different flowrates for each conditioner with the flowrate of the LDV tests (approximately 40 l/s) being in the middle of the range. The results below are average values weighted towards the higher flow rates where differential pressure can be measured with less uncertainty.

Plate	MHI	U. Laws	C. Laws	NEL
K	1.2	0.8	1.3	2.9

Note that the unchamfered Laws conditioner has a lower head loss than the chamfered Laws conditioner as it has a far greater porosity value. The application of an upstream chamfer will help to reduce the relatively large value of K for the Spearman (NEL) conditioner.

6. Final conclusions

LDV has been used to measure axial velocity and *r.m.s.* fluctuation velocity profiles downstream of four perforated plate flow conditioners which have been placed $4D$ downstream of a single 90° swept bend and a twisted S bend in turn. Measurements, without the insertion of a flow conditioner, were made downstream of the flow-disturbing installations for comparison. By comparing the velocity profiles against a baseline profile, with tolerance limits of $\pm 5\%$ similar to ISO 5167-1 Clause 7.4., it was found that the Spearman (NEL) conditioner produced profiles that met the tolerance limits from $11D$ downstream of the conditioner for the single bend and $6D$ downstream of the conditioner for the twisted S bend. Whereas the single bend result could be matched by other conditioners the twisted S bend result could not. From this result the original objective of the project has been achieved in that a perforated plate flow conditioner has been designed that has a performance at least as good as any other design. It has also been shown that significant reductions in the required lengths of pipe in ISO 5167-1 can be made with a variety of perforated plate designs. Further testing is being undertaken, and it is hoped that the Spearman (NEL) design can be introduced into the various flow metering standards for the benefit of flowmeter users.

Acknowledgements

The work reported here was done with the support of the Standards, Quality and Measurement Advisory Committee of the Department of Trade and Industry. The authors would like to thank Dr E. Laws for providing drawings of the two Laws conditioners tested, as well as Mr I. G. Nicholson and Mrs L. A. Johnstone for their help during the differential pressure tests.

References

- 1 International Organization for Standardization. Measurement of fluid flow by means of orifice plates, nozzles and Venturi tubes inserted in circular cross-section conduits running full. ISO 5167-1, Geneva: International Organization for Standardization, 1991.
- 2 British Standards Institution. Measurement of fluid flow in closed conduits. Part 1: Pressure differential devices. Section 1.1. Specification for square edged orifice plates, nozzles and Venturi tubes inserted in circular cross-section conduits running full. BS 1042: Part 1: Section 1.1, 1992.
- 3 Zanker, K. J., The development of a flow straightener for use with orifice plate flowmeters in disturbed flows. BHRA paper No SP 625. Harlow: British Hydromechanics Research Association, 1959.
- 4 Kinghorn, F. C., McHugh, A. and Dyet, W. D., The use of Etoile flow straighteners with orifice plates in swirling flow. ASME publication 79-WA/FM-7. Presented at the Winter Meeting, New York, December 1979.
- 5 Humphreys, J. S. and Hobbs, J. M., An investigation of the effectiveness of flow conditioners. In *Proc. of Int. Symp. on Fluid Flow Measurement*. Washington DC: American Gas Association, November 1986, pp. 883–897.
- 6 Akashi, K., Watanabe, H. and Koga, K., Development of new rectifier for shortening upstream pipe length of a flowmeter. *Proceedings of IMEKO Symposium 'Flow measurement and control in Industry'*, Tokyo, 1979, pp. 279–284.
- 7 Laws, E. M., Flow conditioning—a new development. *Flow Meas. Instrum.*, 1990, **1**(3), 165–170.
- 8 Elder, J. W., Steady flow through non-uniform gauzes of arbitrary shape. *J. Fluid. Mech.*, 1958, **5**, 355–368.
- 9 Sanderson, M. L. and Sweetland, D., The effect of four designs of flow conditioner on flowmeter performance. *Flow Measurement and Instrumentation Consortium, Category 2A Report No. 1*. Cranfield, Bedford: Cranfield Institute of Technology, July 1991.
- 10 Lake, W. T. and Reid, J., Optimal flow conditioner. In *Proc. of North Sea Flow Measurement Workshop*, Peebles, Paper No. 1.3. East Kilbride, Glasgow: NEL, October 1992.
- 11 British Standards Institution. Measurement of fluid flow in closed conduits. Part 2: Velocity area methods. Section 2.1. Method using pitot static tubes. BS 1042: Part 2: Section 2.1: 1983.
- 12 Mattingly, G. E. and Yeh, T. T., Effects of pipe elbows and tube bundles on 50 mm orifice meters. *Symposium on Installation Effects on Flow Metering*, Paper No. 3.1. East Kilbride, Glasgow: NEL, October 1990.
- 13 Karnik, U., Jungowski, W. M. and Botros, K. K., Effects of turbulence on orifice meter performance. *J. Offshore Mechanics and Arctic Engng*, 1994, **116**, 77–85.
- 14 Karnik, U., Measurements of the turbulence structure downstream of a tube bundle at high Reynolds numbers. *J. Fluids Engng*, 1994, **116**, 848–855.
- 15 Laufer, J., The structure of turbulence in fully-developed pipe flow. National Advisory Committee for Aeronautics, USA, Report 1174, 1954.